Chapter 4

Synthesis and Characterization and Biological Evolution of Zinc(II) Metal Complexes of 4-Semicarbazone-5-Pyrazolone and 4-Thiosemicarbazone-5-Pyrazolone

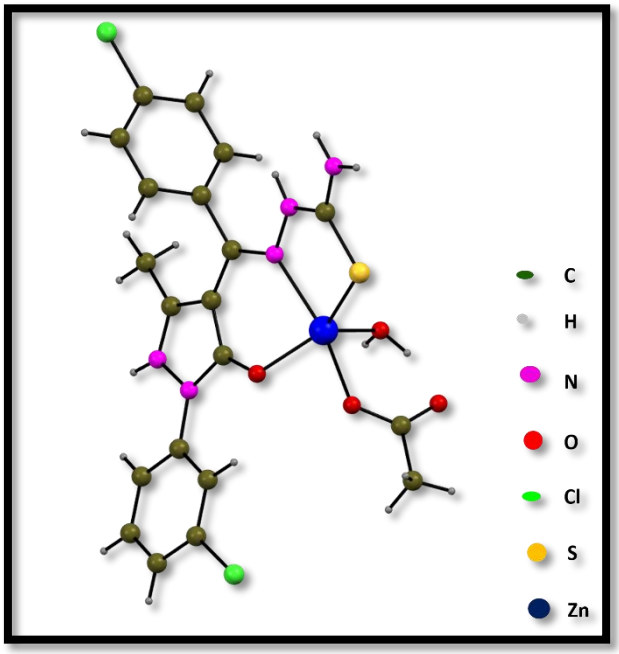

4.1. Introduction

Since many years, pyrazolone based derivatives have grabbed the attention of the researcher, as they can easily form and more applications in drug, dyes and coordination chemistry.[1–4] 4-acyl pyrazolone and their derivatives have gained the considerable interest of researchers, in the field of coordination chemistry.[5–10] In the coordination chemistry 4-acyl pyrazolone based ligands rapidly becoming popular for use in many biological applications, dyes and catalysis.[2]

4-semicarbazone and metal complexes

4-semicarbazone are prepared by condensation of the corresponding 4-acyl-pyrazolones and the desired Semicarbazide. Semicarbazide available in Semicarbazide hydrochloric acid, hence first to neutralize with base and used in the reaction with a ketone. In the case of 4-semicarbazone-5-pyrazolone very useful in coordination chemistry due to their tautomerism and they have reacted as a monoanionic or a dianionic with the metal ion, tautomerism forms of 4-semicarbazone-5-pyrazolone have been displayed in the chart 4.1.[11]

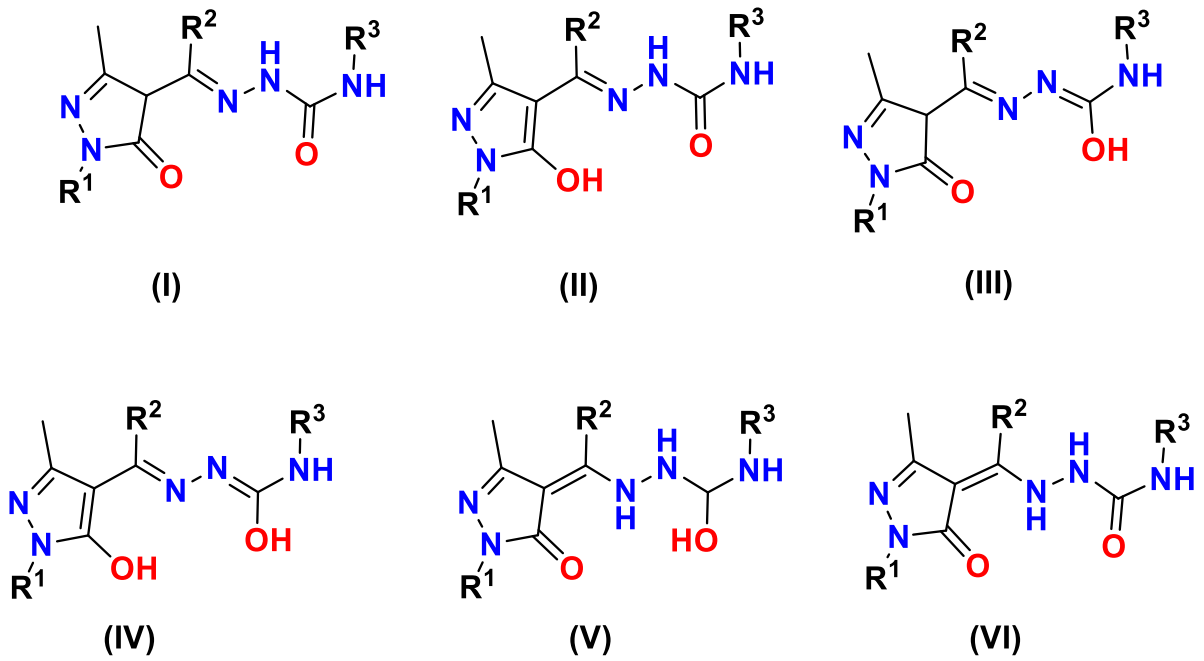

Chart 4.1. Tautomers of 4-semicarbazone-5-pyrazolones. R^1 = substituted phenyl group, R^2 = aryl or an alkyl group and R^3= - H or aryl group.

4-thiosemicarbazone and metal complexes

The 4-thiosemicarbazone-5-pyrazolone synthesis by refluxing an appropriate amount of respective 4-acyl pyrazolone with the thiosemicarbazide in ethanol.[12] As a ligand 4-thiosemicarbazone-5-pyrazolone behaved as tridentate mono anion ONS donor molecules.[13] The coordination ability of the thiosemicarbazone derivatives of AP have been proved in complexation reaction with Cu(II), Ni(II) and Co(II) ions.[14]

4.2. Experimental

4.2.1. Material and method

Pyrazolones were obtained from Sidhdhanath industries, Sachin (Surat), India as gift samples. All necessary reagents and solvents were obtained from commercial sources. Zinc acetate, glacial acetic acid, Semicarbazide and thiosemicarbazide were purchased from Loba chem, SD fine and spectrochem PVT. LTD., Mumbai. Infrared (IR) spectra were recorded on Bruker Alpha Fourier transform IR (FT-IR) spectrometer as KBr pellets. ^{1}H NMR spectra of the ligand were recorded with an AV 400 MHz Bruker FT-NMR instrument. Single crystal data were collected on an Xcalibur, EOS, Gemini diffractometer. The electronic spectrum was recorded on a Perkin Elmer Lambda 35 UV-Vis spectrometer. A simultaneous TG/DTA was carried out on an SII EXSTAR6000 TG/DTA 6300 instrument. The experiments were performed in N_2 at a heating rate of 10 ºC min^{-1} in the temperature range 30–550 ºC using an aluminium pan. Gravimetric and volumetric analysis were performed for the determination of zinc after decomposition of the complex in nitric acid.

4.2.2. Synthesis of ligands

4-acyl pyrazolones **L2** and **L3** were synthesized as followed as chapter **2a** method.

4.2.2.1. Synthesis of ligand L7 [(E)-2-((4-chlorophenyl)(1-(3-chlorophenyl)-5-hydroxy-3-methyl-1H-pyrazol-4-yl)methylene)hydrazine-1-carboxamide].

In the ligand preparation, Semicarbazide hydrochloric acid (0.002 mol, 0.223 g) was dissolved in anhydrous ethanol and added sodium hydroxide (0.002 mol, 0.08 g) for neutralization. Followed by the added ethanolic solution of **L2** (0.002 mol, 0.694 g) with constant stirring. 1 mL of acetic acid was added in the reaction mixture as a catalyst. After that refluxed the reaction mixture for 4 h. Cool the reaction mixture to room temperature after the reaction, the yellowish precipitates were formed. Filtrated by simple filtration method and washed with cool

ethanol and air-dried. Yield: 75 %, M.P.:185 °C, Mol. Formula: $C_{18}H_{15}Cl_2N_5O_2$, F.w.: 404.25, Elem. Ana., Theoretical (found) %: C, 53.48 (53.40); H, 3.74 (3.88); N, 17.32 (17.87). **FTIR(KBr, cm^{-1})**: 3412, 3207 (N-H, scz), 1670 (C=O, pyz), 1629 (C=O, scz), 1590 (C=N, pyz). **^{1}H NMR(400 MHz, $CDCl_3$, δ ppm):** 2.13 (s, CH_3-pyz), 3.15 (s, 1H, NH), 7.19-7.96 (m, 6H, semi-pyz).

4.2.2.2. Synthesis of ligand L8 ((E)-2-((4-chlorophenyl)(5-hydroxy-3-methyl-1-(p-tolyl)-1H-pyrazol-4-yl)methylene)hydrazine-1-carboxamide)

In the ligand **L8** preparation, the method was as same as ligand **L7**, a change is **L3** (0.002 mol,0.652 g) was used in place of L2. Yield: 74 %, M.P.:188°C, Mol. Formula: $C_{19}H_{18}ClN_5O_2$, F.w.: 383.84, Elem. Ana. Theoretical (found): C, 59.45(58.99); H, 4.73(4.74); N, 18.25(18.55). **FTIR (KBr, cm^{-1})**: 3470 (N-H, scz), 1679 (C=O, pyz), 1600 (C=O, scz), 1565 (C=N, pyz). **^{1}H NMR (400 MHz, $CDCl_3$, δ ppm):** 1.26(s, 3H, CH_3-tolyl), 2.13 (s,3H, CH_3-pyz), 7.28-7.30(d, 2H, *p*-tolyl), 7.51-7.62(dd, 4H, *p*-chloro benzoyl), 7.71-7.73(d, 2H, *p*-tolyl). Synthesis route of ligands **L7** and **L8** displayed in scheme 4.1.

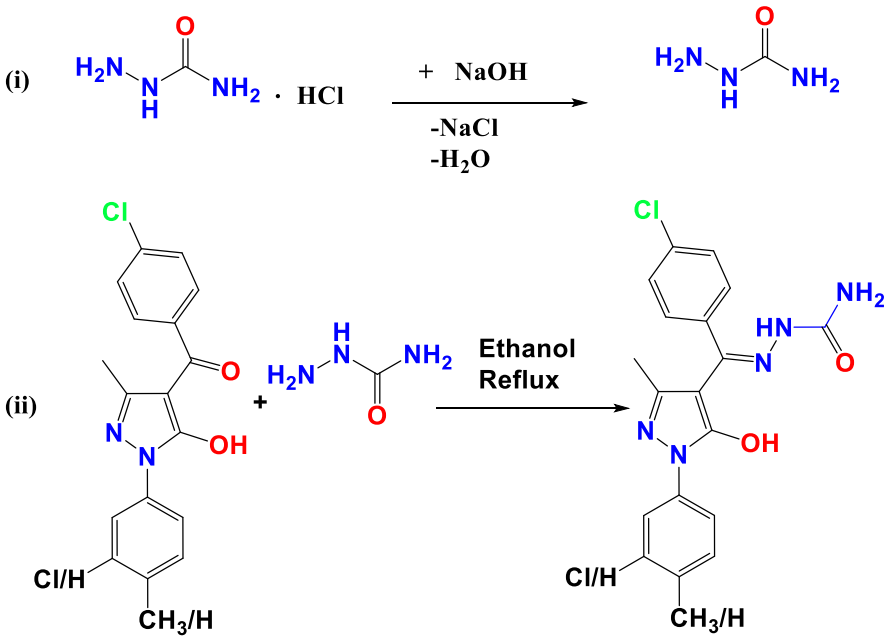

Scheme 4.1. Synthesis route of ligands **L7** and **L8**.

4.2.2.3. Synthesis of ligand L9 ((E)-2-((4-chlorophenyl)(1-(3-chlorophenyl)-5-hydroxy-3-methyl-1H-pyrazol-4-yl)methylene)hydrazine-1-carbothioamide)

In the ligand **L9** preparation, Thiosemicarbazide (0.002 mol, 0.182 g) was dissolved in anhydrous ethanol (25 ml) in a 100 mL single neck RBF. Followed by the dropwise added ethanolic solution of L2 (0.002 mol, 0.694 g) in RBF. A few drops of glacial acetic acid added in the reaction mixture as a catalyst and refluxed for 4 h. Resulted in yellow precipitates were filtered by the simple filtration method. Yield 67%, M.P.:174°C, Mol. Formula: $C_{18}H_{15}Cl_2N_5OS$, F.w.: 420.31, Elem. Ana. Theoretical (found): C, 51.44(51.45); H, 3.60(3.77); N, 16.66(16.77); S, 7.63(7.68). **FTIR (KBr, cm^{-1})**: 3331(N-H, tcz), 1662 (C=O, pyz), 1602 (C=N, tcz), 831 (C=S, tcz). **^{1}H NMR (400 MHz, $CDCl_3$, δ ppm):** 2.2 (s, 3H, CH_3-pyz), 7.30-7.31(d, 1H, m-ch-p), 7.39-7.43(t, 1H, m-ch-p), 7.51-7.63(dd, 4H, *p*-chloro-benz), 7.9(s, 1H, m-ch-p).[15]

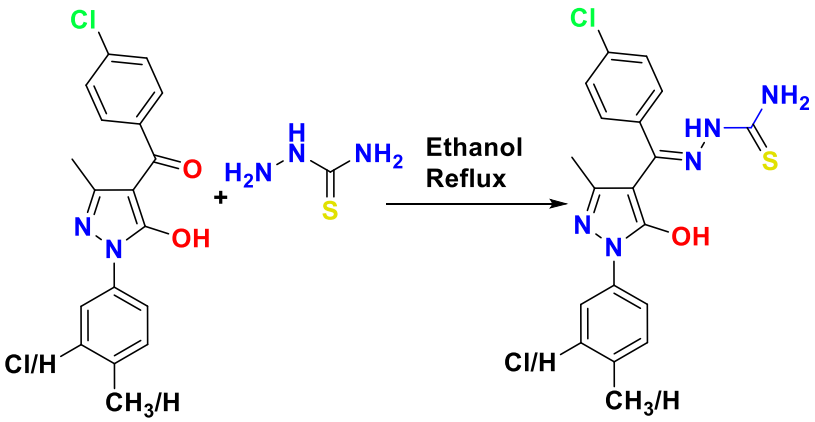

Scheme 4.2. Synthesis route of ligand **L9** and **L10**.

4.2.2.4. Synthesis of ligand L10 ((E)-2-((4-chlorophenyl)(5-hydroxy-3-methyl-1-(p-tolyl)-1H-pyrazol-4-yl)methylene)hydrazine-1-carbothioamide)

In the ligand **L9** preparation, Thiosemicarbazide (0.002 mol, 0.182 g) was dissolved in anhydrous ethanol (25 ml) in a 100 mL single neck round bottom flask. Followed by the dropwise added ethanolic solution of **L3** (0.002 mol, 0.652 g) in the flask. A few drops of glacial acetic acid were added in the reaction mixture as a catalyst and refluxed for 4 h. Resulted in yellow precipitates were filtered by the simple filtration method. Yield 77%, M.P.:185°C, Mol. Formula: $C_{19}H_{18}ClN_5OS$, F.w.: 399.90. Elem. Ana. Theoretical (found): C, 57.07(57.14); H, 4.54(4.64); N, 17.51(17.55); S, 8.02 (8.88). **FTIR (KBr, cm^{-1})**: 3388 (N-H, scz), 1670

(C=O, pyz), 1547 (C=N, pyz), 859 (C=S, tcz). **^{1}H NMR (400 MHz, $CDCl_3$, δ ppm):** 2.1 (s, 3H, CH_3-*p*-tolyl), 2.4 (s, 3H, CH_3-pyz), 7.28-7.30(d, 2H , tolyl), 7.49-7.62 (dd, 4H, p-chloro benzoyl), 7.71-7.73(d, 2H, pyz).

4.2.3. Synthesis of complexes 19-22

4.2.3.1. Synthesis of complex 19 $[Zn(L7)_2]$

Dissolved the ligand **L7** (0.001 mol, 0.420 g) in a minimum amount of methanol in single neck round bottom flask. Followed by the dropwise added methanolic solution of zinc acetate dehydrate (0.0005 mol, 0.109 g) in the solution of the ligand with constant stirring. After half an hour added a methanolic solution of sodium acetate. The reaction mixture was refluxed for 4 h. Off white precipitates were obtained. The final product was filtered and washed with methanol and hot water. Yield: 75 %. M.p.: >200 °C. Anal. calcd. for $C_{36}H_{28}Cl_4N_{10}O_4Zn$: C, 49.59; H, 3.24; N, 16.07; Zn, 7.50. Found: C, 49.50; H, 3.55; N, 16.74%. F.w. 871.87, metal estimation: 7.55 %. FT-IR (KBr, cm^{-1}): 3358 (b) (NH-),3181 (NH_2), 2927 (b) (Ph–C–H), 1662 (C=O, scz), 1602 (C=N, cyclic), 1549 (C=N, azomethine), 1482 (m) (Ph-C-C), 867 (s) (N-N), 511 (s) (Zn–O), UV/Vis (DMSO, λmax, nm, (ε)): 275 (0.85). Λ_m ($S.cm^2.mol^{-1}$): 8.2.

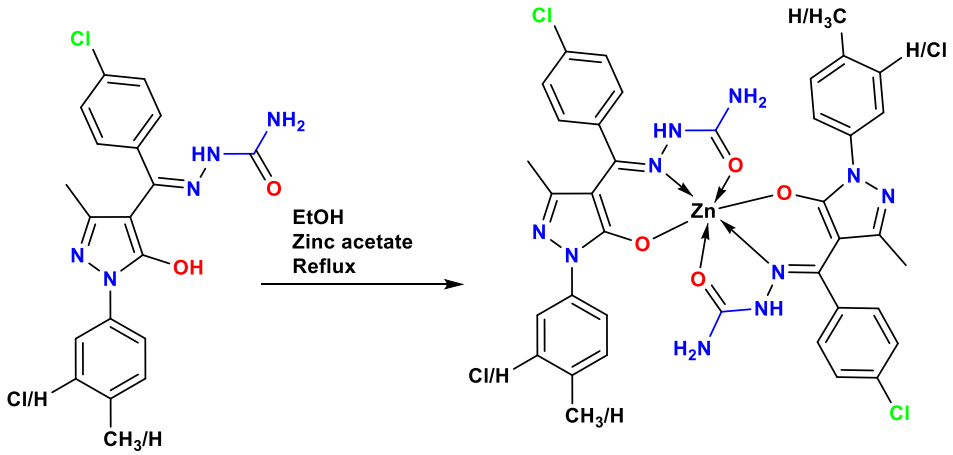

Scheme 4.3. Synthesis route of complex **19** and **20**.

4.2.3.2. Synthesis of complex 20 $[Zn(L8)_2]$

The procedure for the preparation of complex **20** is similar to that for complex 19 except for the replacement of ligand **L7** with ligand **L8**.

Yield: 58 %. M.p.: >200 °C. Anal. calcd. for $C_{38}H_{34}Cl_2N_{10}O_4Zn$: C, 54.92; H, 4.12; N, 16.85. Found: C, 55.36; H, 4.05; N, 16.77%. Metal estimation 7.88%. F.w.: 831.04. FTIR (KBr, cm^{-1}): 3388 (b) (NH-),3155 (b) (NH_2), 2923 (b) (Ph–C–H), 1669(C=O. scz), 1556 (m) (C=N, cyclic), 1435 (m) (Ph-C-C), 1127 (m) (N-N), 859 (s) (N-N), 514 (s) (Zn–O). UV/Vis (DMSO, λmax, nm, (ε)): 287 (0.84). Λ_m ($S.cm^2.mol^{-1}$): 4.2. synthesis route of complex **19** and **20** depictred in scheme 4.3.

4.2.3.3. Synthesis of complex 21 [Zn(L9)(OAc)(H_2O)](EtOH)

The ligand **L9** was dissolved in methanol in single neck 100 ml round bottom flask. Followed by dropwise added methanolic solution of zinc acetate dihydrate in the ligand solution. The pinch of sodium acetate was added in the mixture and refluxed for 4 h. the resulting solution was allowed to cool in room temperature and the light yellow precipitates was collected by simple filtration, washed with ethanol and air-dried. Yield: 66 %. M.p.: >200 °C. Anal. calcd. for $C_{22}H_{25}Cl_2N_5O_5SZn$: C, 43.47; H, 4.15; N, 11.52. Found: C, 43.36; H, 3.95; N, 11.75%. FT-IR (KBr, cm^{-1}): 3402 (b) (NH-),3159 (b) (NH_2), 2927 (b) (Ph–C–H), 1612 (C=N, pyz), 1589 (m) (C=N, cyclic), 1474 (m) (Ph-C-C), 1139 (m) (N-N), 1015 (m) (C=S), 862 (s) (N-N), 511 (s) (Zn–O), 480 (s) (Zn–N), 445 (s) (S-O). **^{1}H NMR (400 MHz, DMSO-d6, δ ppm):** 1.9 (s, 3H, CH_3, pyz), 7.11-7.13(d, 1H, *m*-chloro phenyl), 7.16-7.23 (m, 4H, Ar-H), 7.39-7.43(t, 2H, m-chloro phenyl), 7.47-8.32(4H, Ar-H).UV/Vis (DMSO, λmax, nm, (ε)): 288 (0.6). Λ_m ($S.cm^2.mol^{-1}$): 3.3.[15] Synthesis route of complex 21 is depicted in Scheme 4.4.

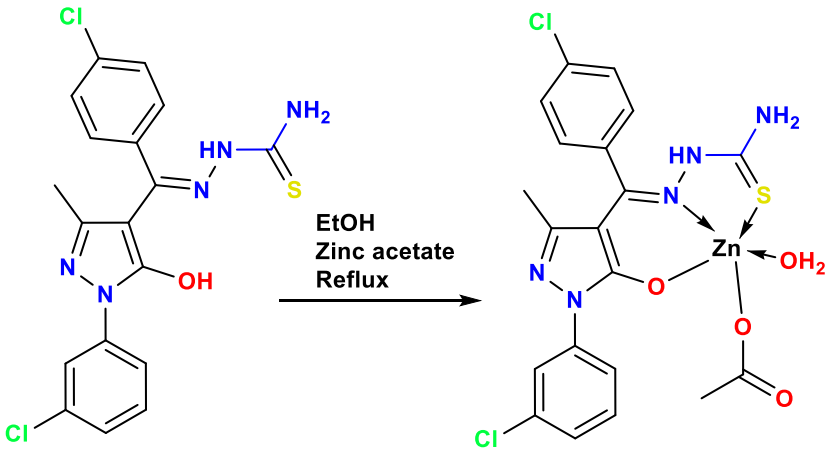

Scheme 4.4. Synthesis route of complex 21.

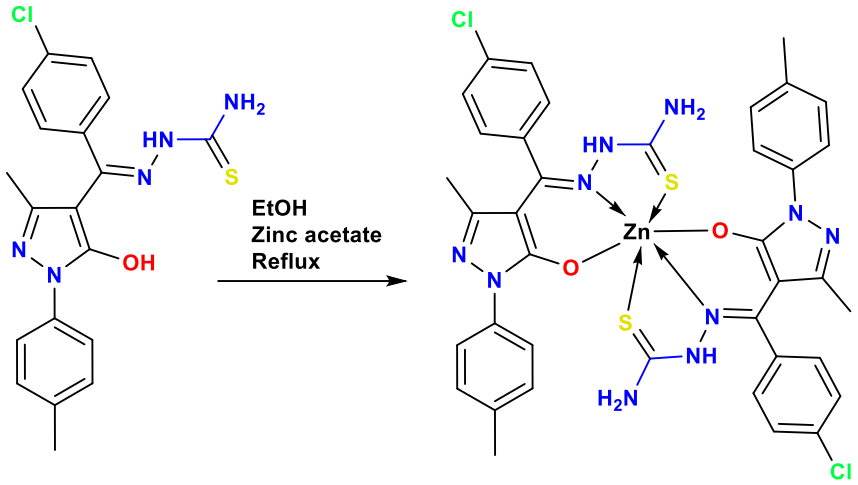

Scheme 4.5. Synthesis route of complex 22.

4.2.3.4. Synthesis of complex 22 [Zn(L10)$_2$]

The procedure for the preparation of complex **22** is similar to that for complex **21** except for the replacement of ligand **L9** with ligand **L10**.

Yield: 65 %. M.p.: >200 °C. Anal. calcd. for $C_{38}H_{34}Cl_2N_{10}O_4Zn$: C, 54.92; H, 4.12; N, 16.85. Found: C, 54.34; H, 4.22; N, 16.88%. Metal estimation 7.88 %. FT-IR (KBr, cm^{-1}): 3423 (b) (NH-),3038 (b) (NH_2), 2977 (b) (Ph–C–H), 1597 (C=O, pyz) 1565 (m) (C=N, cyclic), 1478 (m) (Ph-C-C)), 1160 (C=N, azomethine), 855 (s) (N-N), 1016 (m) (C=S), 511 (s) (Zn–O), 480 (s) (Zn–N), 445 (s) (S-O). **^{1}H NMR (400 MHz, $CDCl_3$, δ ppm):** 1.7 (s, 3H, CH_3-*p*-tolyl), 2.3 (s, 3H, CH_3-pyz), 7.08-7.77(8H , Ar-H). UV/Vis (DMSO, λmax, nm, (ε)): 287 (0.84). Λ_m ($S.cm^2.mol^{-1}$): 8.5. Synthesis route of complex 22 is depicted in scheme 4.5.

4.2.4. Single crystal X-ray diffractions

The X-ray single crystal data of ligand **L8** and a complex **21** were collected on an Xcalibur, EOS, Gemini diffractometer with graphite monochromatic MoKα radiation (λ= 0.71073Å). All structures were solved by direct methods using SHELXS-97[16] and refined by the full-matrix least-square method based on F2 using the SHELXL-2018 program.[17] All crystallographic calculations were done with the Olex2 GUI.[18] The geometries of the molecules were determined using the software PLATON[19] and PARST [20]. All structures were solved by direct methods and refined in a regular pattern.[16,21] Graphics of **L8** and complexes **21** were generated using MERCURY (version 4.1.0) software.[22] In all the cases, non-hydrogen atoms were treated anisotropically. The hydrogen atoms were geometrically fixed. The crystallographic parameters for ligands and complex are tabulated in Table 4.1.

Table 4.1. Crystal data and structure refinement for ligand L8 and complex 21

Identification code	L8	Complex 21
Empirical formula	$C_{19}H_{18}ClN_5O_2$	$C_{22}H_{26}Cl_2N_5O_5SZn$
Formula weight	383.84	608.81
Temperature/K	293(2)	273.0
Crystal system	monoclinic	Triclinic
Space group	Cc	P-1
a/Å	18.350(2)	8.1030(7)
b/Å	11.587(2)	12.1220(10)
c/Å	9.1401(14)	14.9628(12)
α/°	90	72.777(7)
β/°	100.786(13)	75.541(7)
γ/°	90	88.486(7)
Volume/Å^3	1909.1(5)	1357.5(2)
Z	22	2
ρ_{calc}g/cm^3	1.335	1.489
μ/mm^{-1}	0.224	1.220
F(000)	800.0	626.0
Crystal size/mm^3	0.3× 0.1×0.1	0.3 × 0.2 × 0.2
Radiation	MoKα (λ = 0.71073)	MoKα (λ = 0.71073)
2Θ range for data collection/°	6.474 to 58.264	6.128 to 57.92
Index ranges	-24 ≤ h ≤ 24, -15 ≤ k ≤ 15, -11 ≤ l ≤ 12	-10 ≤ h ≤ 10, -14 ≤ k ≤ 15, -11 ≤ l ≤ 20
Reflections collected	10796	6488
Independent reflections	*4385 [R_{int} = 0.0667, R_{sigma} = 0.0933]*	*5415 [R_{int} = 0.0196, R_{sigma} = 0.0554]*
Data/restraints/parameters	4385/2/247	5415/0/330
Goodness-of-fit on F^2	0.998	1.030
Final R indexes [I>=2σ (I)]	*R_1 = 0.0625, wR_2 = 0.1367*	*R_1 = 0.0489, wR_2 = 0.1130*
Final R indexes [all data]	*R_1 = 0.1536, wR_2 = 0.1889*	*R_1 = 0.0703, wR_2 = 0.1281*
Largest diff. peak/hole / e Å^{-3}	0.16/-0.24	0.96/-0.84
Flack parameter	-0.01(9)	-
CCDC	2048411	1906438

4.2.5. MTT cell viability assay

A549 (human lung carcinoma) cells were procured from National Centre of Cell Sciences, Pune, India. Cells were maintained at 37 °C and 5% CO_2. Cells were seeded (1×105 cells) in a T25 flask and cultured in DMEM containing 10% FBS and 1% antibiotic-antimycotic solution with trypsinization at every third day and sub-culturing with a TPVG solution. 1 mg test complex was dissolved in 5 µL DMSO solvent and later, 1, 5, 10, 25, 50, 100, 200, 500 and 1000 µg/mL doses were tested against A549 cells for cytotoxicity using 3-(4,5-dimethyl-thiazol-2-yl)-2,5-diphenyltetrazolium bromide (MTT) cytotoxicity assay. A549 cells (7×103 cells/well) were seeded in 96-well culture plates (Tarson India Pvt. Ltd.) for 24 h in the absence or presence of the complex. Later, 10 µL MTT (5 mg/mL) was added to the wells and plates were incubated at 37 °C for 4 h to form the formazan crystals. The culture media was discarded and wells were washed with PBS. The resultant formazan was dissolved in 150 µL of DMSO and absorbance was read at 540 nm in Synergy HX-Multimode Reader (Biotek, USA).

4.3. Results and discussion

In this chapter, four zinc(II) complexes have been prepared by following the scheme 4.6 described below;

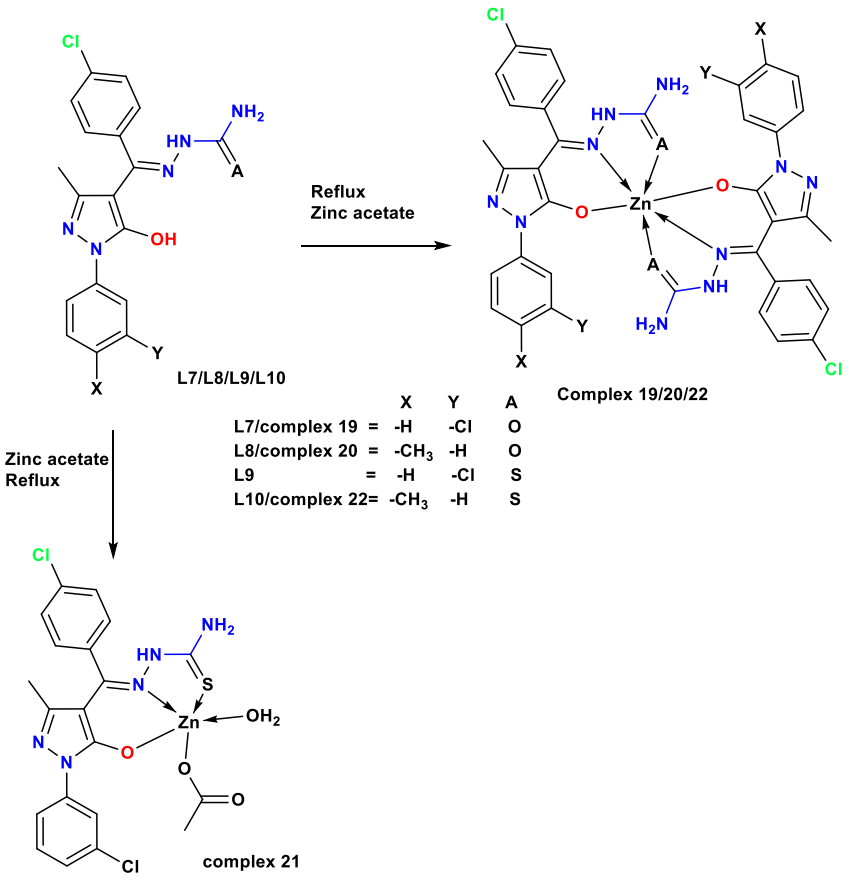

Scheme 4. 6. Synthesis route of complexes **19-22.**

All these complexes are light yellow solid , stable at room temperature and soluble in DMF and DMSO.

The detailed characterization of these complexes is described in succeeding sections.

4.3.1. Single crystal X-ray diffraction

4.3.1.1. Single crystal X-ray diffraction of ligand L8.

The molecular structure of ligand **L8** was determined by single crystal X-ray diffraction. Selected bond length and bond angles are given in Table 4.2. The structure with the numbering scheme is shown in Fig. 4.1 and the crystallography data are presented in Table 4.1.

Bond distance reveals that the bond nature in the structure, specially C8-O1 and C19-O2 bond distances are 1.255 and 1.212 Å respectively, which values are very similar to C=O.[23] Bond distance of C10-N2 and C12-N3 are 1.318(8) and 1.317(8) Å respectively, which indicates the double bond between C and N in the ligand molecule. C9-C10 bond distance shows 1.414 Å which confirms a single bond. Furthermore, C19-N4 bond distance shows 1.355(8) Å which confirm a single bond.

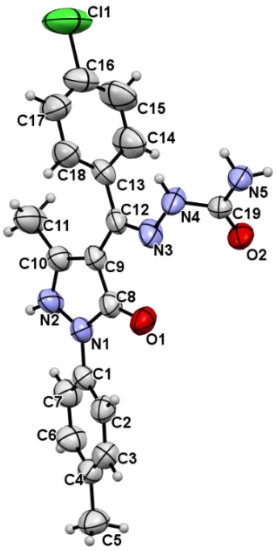

Fig. 4.1. ORTEP ellipsoid diagram of ligand **L8** with 50% probability. Small **s**pherical are H-atoms of the molecules.

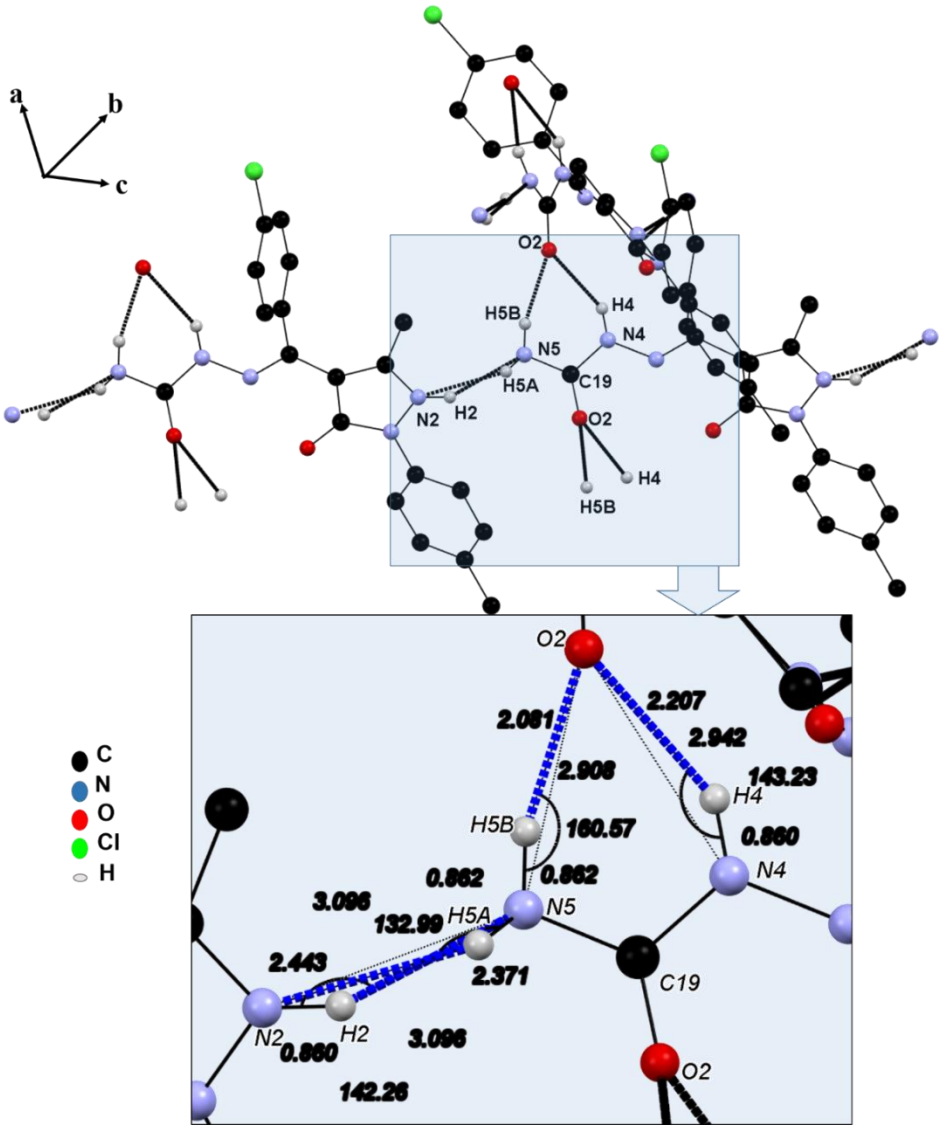

Fig. 4.2. Intermolecular H-bond in the ligand **L8** molecule.

The ligand (**L8**) having three intemolecular H-bond in the crystal packing. H-bond parameters are given in table 4.3 and H-bond diagram is depicted in Fig. 4.2.

As per the X-ray diffraction results, ligand **L8** was found in the amine-keto form of tautomerism in the solid-state. Ligand **L8** exhibits the intermolecular H-bond between O2 and nitrogen donors H4 and H5B of semicarbazone. H-bonds parameters are displayed in table 4.3. crystal packing of ligand **L8** viewed down the c-axis illustrated in Fig. 4.3.

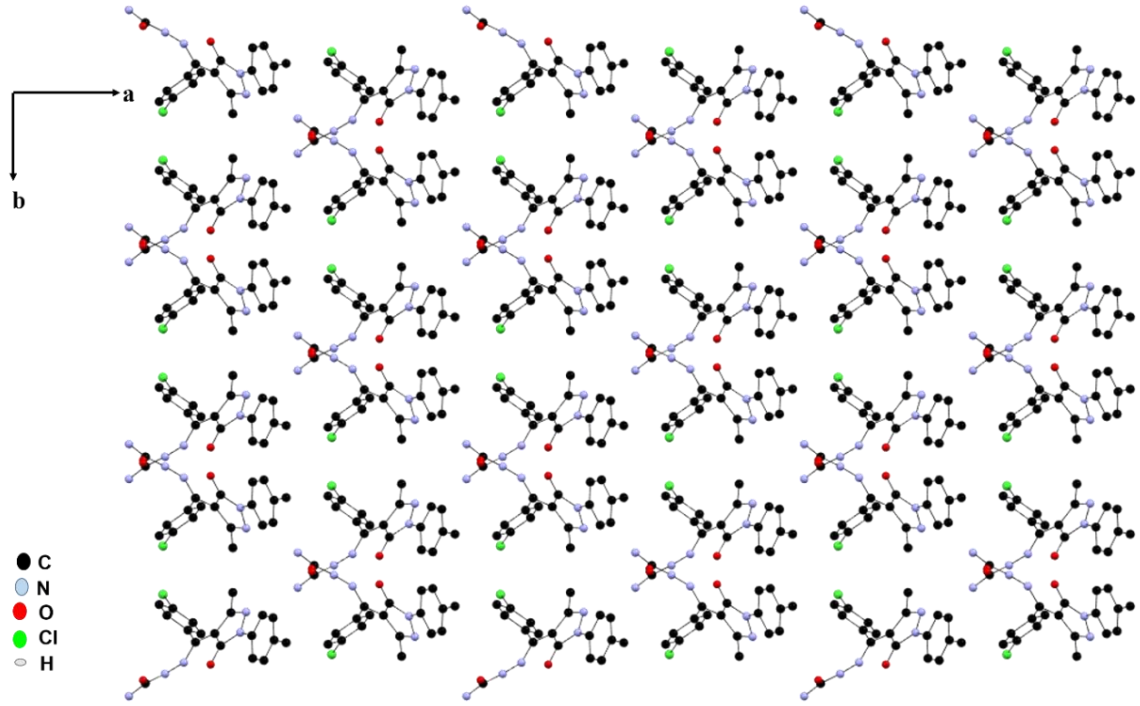

Fig. 4.3. Crystal packing system viewed down from the c-axis.

Table 4.2. Selected bond length and bond angle of ligand **L8**.

Atom	Length/Å	Atom	Angle/°
Cl1-C16	1.745(9)	N2-N1-C1	120.1(5)
O2-C19	1.212(7)	C8-N1-N2	110.9(5)
O1-C8	1.255(8)	C8-N1-C1	128.2(6)
N1-N2	1.385(8)	C10-N2-N1	107.0(5)
N1-C8	1.365(8)	C19-N4-N3	116.1(5)
N1-C1	1.420(8)	C12-N3-N4	121.9(6)
N2-C10	1.318(8)	O1-C8-N1	125.2(6)
N5-C19	1.347(8)	O1-C8-C9	129.1(6)
N4-N3	1.394(7)	N1-C8-C9	105.7(6)
N4-C19	1.355(8)	O2-C19-N5	124.1(6)

Table 4.3. H-bonds parameters of ligand L8 and complex 21.

	D-H…A	(D-H) / Å	(D-A)/ Å	(H…A)/ Å	(D-H-A)/º
Ligand **L8**	N4-H4…O2	0.860	2.942	2.207	143.23
	N5-H5B…O2	0.862	2.908	2.081	160.57
	N5-H5A…N2	0.862	3.096	2.443	132.99
	N2-H2...N5	0.860	3.096	2.371	146.26
Complex 21	N4-H4…O5	0.860	2.992	2.289	139.13
	N5-H5A…O5	0.860	2.826	2.044	150.82
	N5-H5B…O4	0.860	2.997	2.158	165.19
	O2-H2B…O4	0.850	2.688	1.944	145.57

4.3.1.2. Single crystal X-ray diffraction of complex 21.

The molecular structure of the zinc complex and the atom labelling scheme is shown in Fig. 4.4. Selected bond distances and angles are tabulated in Table 4.4.

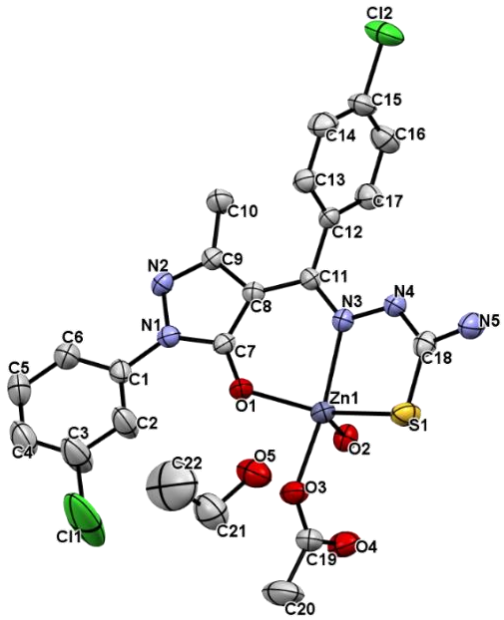

Fig. 4.4. ORTEP ellipsoid with 50% probability diagram of complex **21**. H-atoms are omitted for clarity.

As shown in Fig 4.5, the Zn(II) ion is penta-coordinated by three oxygen atoms of one acyl pyrazolone ligand, one oxygen atom of a water molecule and one oxygen atom of the acetate group. The one oxygen, one thione-sulphur and one azomethine nitrogen of ligand (**L9**) and one oxygen of acetate molecules occupy the basal sites of the square pyramidal structure, whereas the water molecule binds the zinc at the apical site.

In this complex, the combination of the solvent EtOH into the outer-sphere of the complex without coordination bond. The geometry around the zinc(II) ion shows distorted square pyramidal. The zinc atom of complex occupies a distorted square-pyramidal environment (SP), formed by three oxygen atoms [O(1), O(2) and O(3)] supplied by the pyrazolone based ligand, water molecule and acetate molecule respectively. The fourth and fifth coordination sites are occupied by one nitrogen atom and a sulphur atom of ligand (**L9**) molecule. The metal-oxygen distances Zn(1)-O(1), Zn(1)-O(2) and Zn(1)-O(3) are 1.977(2) Å, 2.010(2) Å and 2.090(2) Å respectively. Where the distance between Zn(1)-S(1) shows 2.3293(10) Å and Zn(1)-N(3) displays 2.198(3) Å by the X-ray diffraction study.

In the X-ray diffraction study, complex 21 displays intra-molecular hydrogen bond (O2-H2B···O4) between H2B-O2 of the water molecule and O4 of acetate ion. Second H-bond between H5B-N5 of a ligand molecule and O4 of acetate (Fig. 4.5) is found in the complex. Additional H-bonds of thiosemicarbazone base moiety are ((i) N4-H4…O5 and (ii) N5-H5A…O5) shown in Fig. 4.5. Hydrogen bond parameters are given in Table 4.3.

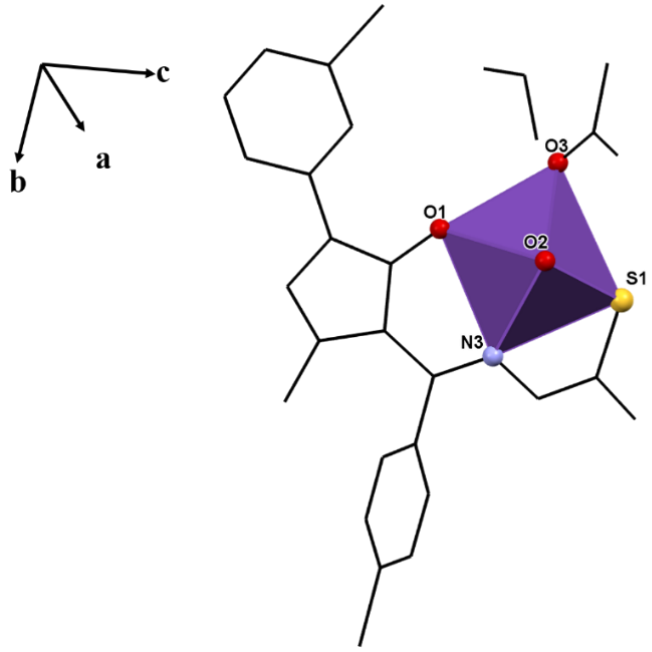

Fig. 4.5. Distorted square pyramidal geometry of complex **21**.

The complex **21** shows distorted square pyramidal geometry around the zinc(II) ion with three oxygen atoms, nitrogen and a sulphur atom. In the geometry, O1, O3, N3 and S1 are in one plane of basal sites and zinc(II) atom stays from the basal plan 0.469 Å. The coordinated Oxygen of water molecule stays 2.476 Å from the basal plan of geometry. The value of the trigonality index τ is 0.299, [$\tau = (\beta - \alpha)/60$), $\beta > \alpha$]. Where α = O1-Zn1–S1 =145.26(8) and β = O3–Zn–N3 = 163.21(10) [τ = 1 for perfect trigonal bipyramidal and τ = 0 for square pyramidal geometries]. Here, the value of trigonality index (τ) indicates geometry around Zn(II) atom can be described as a distorted square pyramidal of complex **21** (*see* Fig. 4.5).[24]

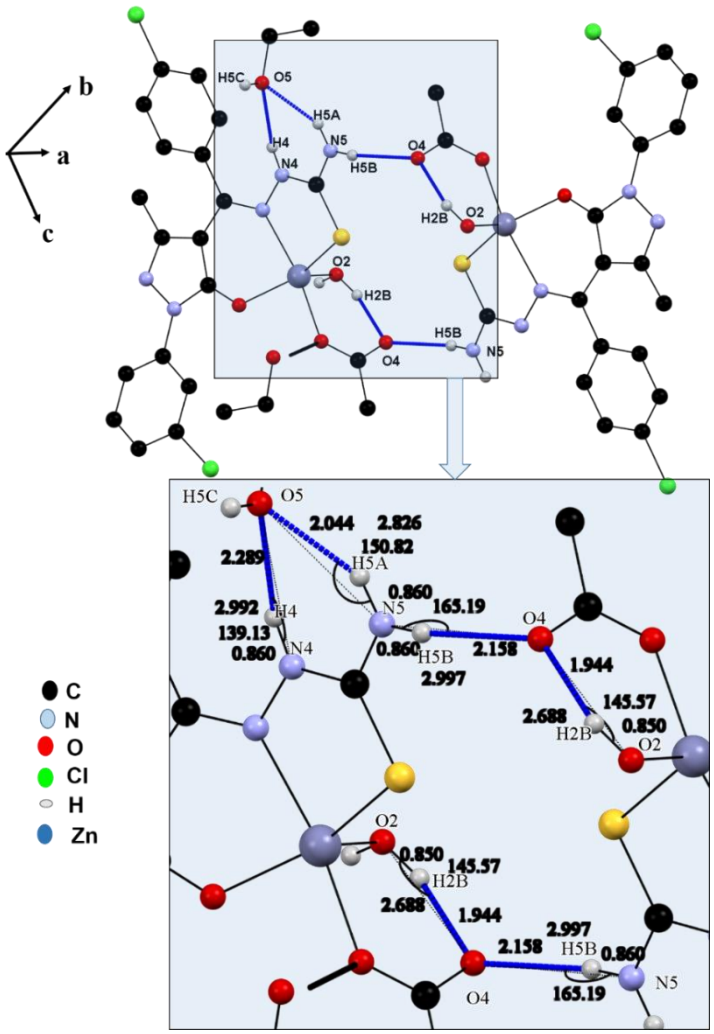

Fig. 4.6. Intermolecular H-bond in the complex 21.

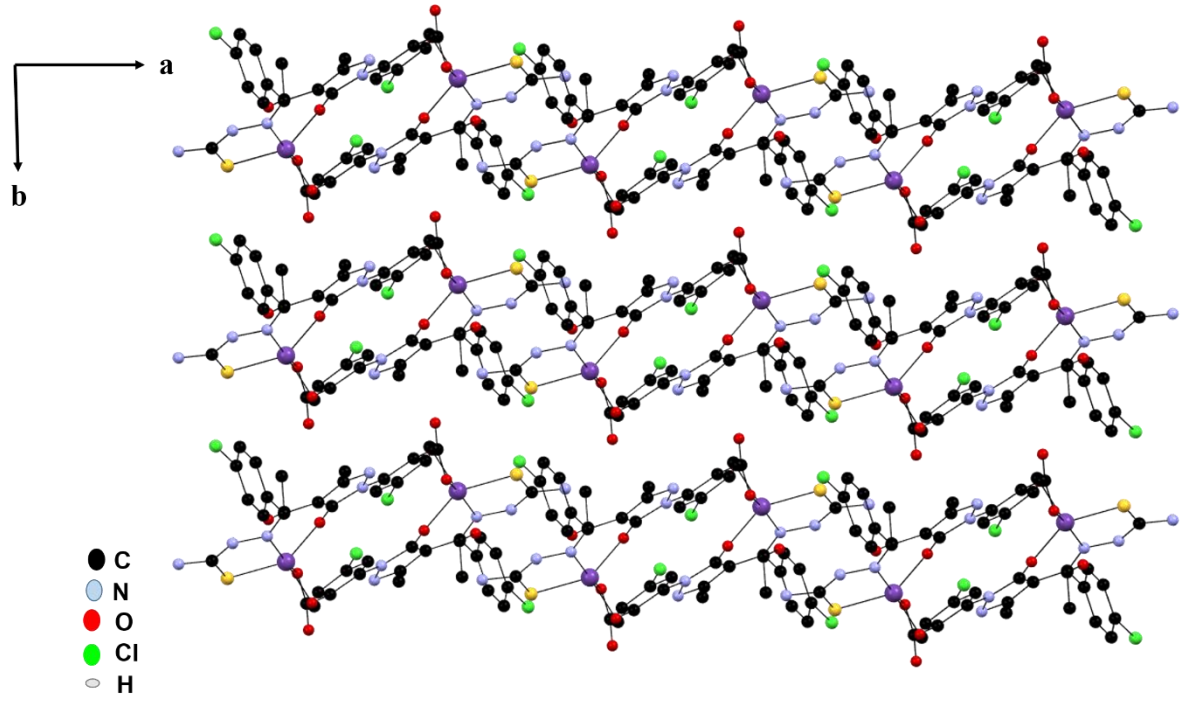

Fig. 4.7. Crystal packing of complex **21** viewed down the c-axis. H-atoms and H-bonds are omitted for clarity (yellow balls indicate sulphur atom).

The zigzag look-alike of crystal packing structure of complex **21**. Crystal packing graphics viewed down the c-axis and comparatively big round shape blue ball indicate zinc atom in the packing.

Table 4.4. Selected bond length and bond angle of complex 21.

Atom	Length/Å	Atom	Angle/°
Zn1-S1	2.3288(10)	O2-Zn1-S1	106.97(8)
Zn1-O2	2.010(2)	O2-Zn1-N3	100.77(10)
Zn1-N3	2.198(3)	O2-Zn1-O3	95.97(10)
Zn1-O1	1.978(2)	N3-Zn1-S1	82.44(7)
Zn1-O3	2.091(2)	O1-Zn1-S1	145.26(8)
S1-C18	1.696(4)	O1-Zn1-O2	107.41(10)
Cl2-C15	1.747(4)	O1-Zn1-N3	86.45(10)
N3-N4	1.385(4)	O1-Zn1-O3	87.21(10)
N3-C11	1.305(4)	O3-Zn1-S1	94.09(8)
N1-C1	1.414(4)	O3-Zn1-N3	163.21(10)
N1-N2	1.384(4)	C18-S1-Zn1	99.25(12)
N1-C7	1.367(4)	N4-N3-Zn1	114.32(19)

O1-C7	1.285(4)	C11-N3-Zn1	127.6(2)
N4-C18	1.346(4)	C11-N3-N4	117.9(3)
C1-C2	1.390(5)	N2-N1-C1	120.0(3)
C1-C6	1.377(5)	C7-N1-C1	129.3(3)
C8-C7	1.406(4)	C7-N1-N2	110.4(3)
C8-C9	1.416(4)	C7-O1-Zn1	122.7(2)
C8-C11	1.430(4)	C18-N4-N3	120.3(3)
C18-N5	1.319(4)	C2-C1-N1	120.6(3)

4.3.2. FTIR spectroscopy of ligands and complexes.

In the FTIR spectrum of ligand **L7**, the spectrum shows a broad peaks at 3470 cm^{-1} of OH and at 3190 cm^{-1} for –NH (amine) of semicarbazone of the ligand moiety. The spectrum shows two sharp peaks at 1670 and 1600 cm^{-1} for amidic ketone and ketone of semicarbazone respectively. The spectrum shows absorbance at 1565 cm^{-1} indicates C=N group in the ligand structure. In the FTIR spectrum of ligand **L8**, the spectrum shows a broad peak at 3470 cm^{-1} of OH and a band shows at 390 cm^{-1} of amine (-NH) of ligand moiety. Two sharp peaks exhibit at 1679 and 1601 cm^{-1} due to the amidic ketone and semicarbazone ketone of the ligand moiety. In the FTIR spectra of ligand **L9** and **L10**, spectra show short absorbance peaks at 3168 and 3151 cm^{-1} for amine (-NH) for ligand **L9** and **L10** respectively. Spectra show a sharp peak at 1662 and 1670 cm^{-1} due to the amidic ketone of **L9** and **L10** respectively. The C=S bond frequency observed at 865 and 859 cm^{-1} of **L9** and **L10** respectively.[15]

In the FTIR spectra of complexes **19** and **20**, spectra show sharp peaks in the range of 1620-1670 cm^{-1} due to a ketone of semicarbazone in complexes **19** and **20** respectively. By the comparison of IR spectra of ligands and complexes, new bands observe in complexes spectra at 1128 cm^{-1} of C-O bond, which indicates ligands were in enolic form in complexation and deprotonation from the C-OH (hydroxyl) group. 443 and 449 cm^{-1} bands indicate M-N bond frequency of complex **19** and **20**. M-O bond frequencies observed in the range of 510-514 cm^{-1} of complexes. In the FTIR spectra of complexes **21** and **22**, spectra 4-thiosemicarbazone-5-pyrazolone based zinc complexes show absorbance frequencies at 862 and 855 cm^{-1} due to the C=S of **21** and **22** respectively. The spectra show bands at 587 and 596 cm^{-1} due to the N-M bonds for **21** and **22** respectively. The spectra display bands at 511 cm^{-1} indicate M-O bonds for both complexes and band observed at 480 and 487 cm^{-1} due to the M-S bond of complex **21** and **22** respectively. FTIR spectra of ligands and complexes are presented in Fig. 4.8 to Fig. 4.15.

FTIR spectra of ligands and complexes

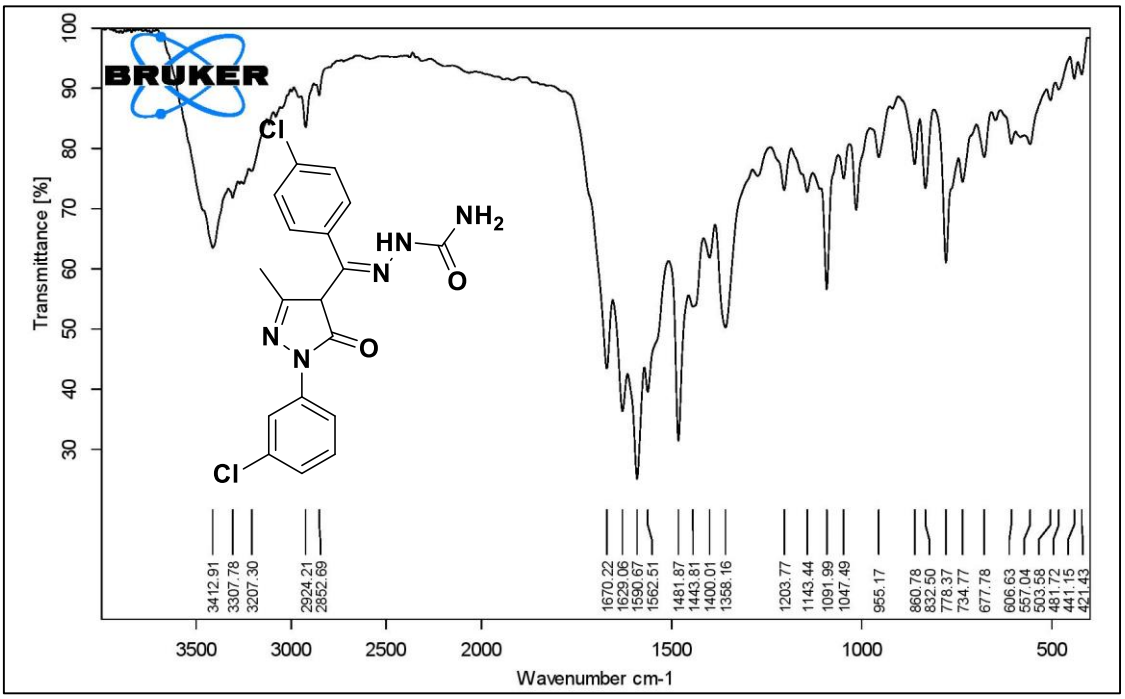

Fig. 4.8. FTIR spectrum of ligand **L7**.

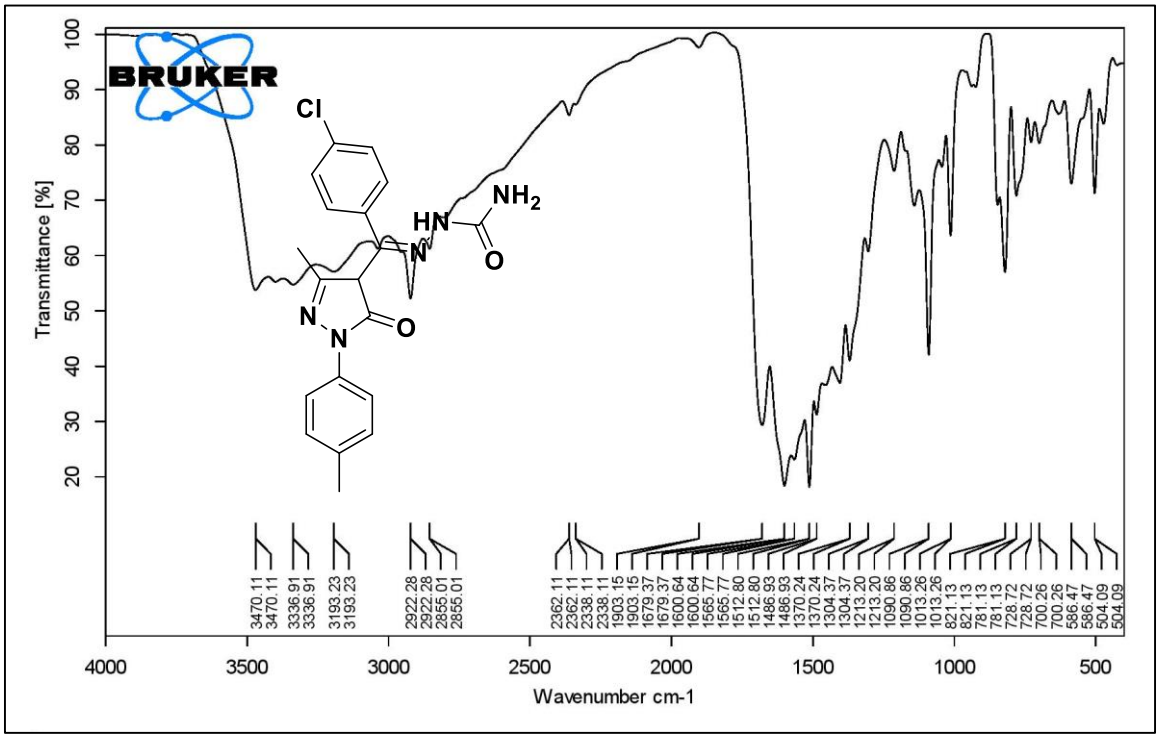

Fig. 4.9. FTIR spectrum of ligand **L8**.

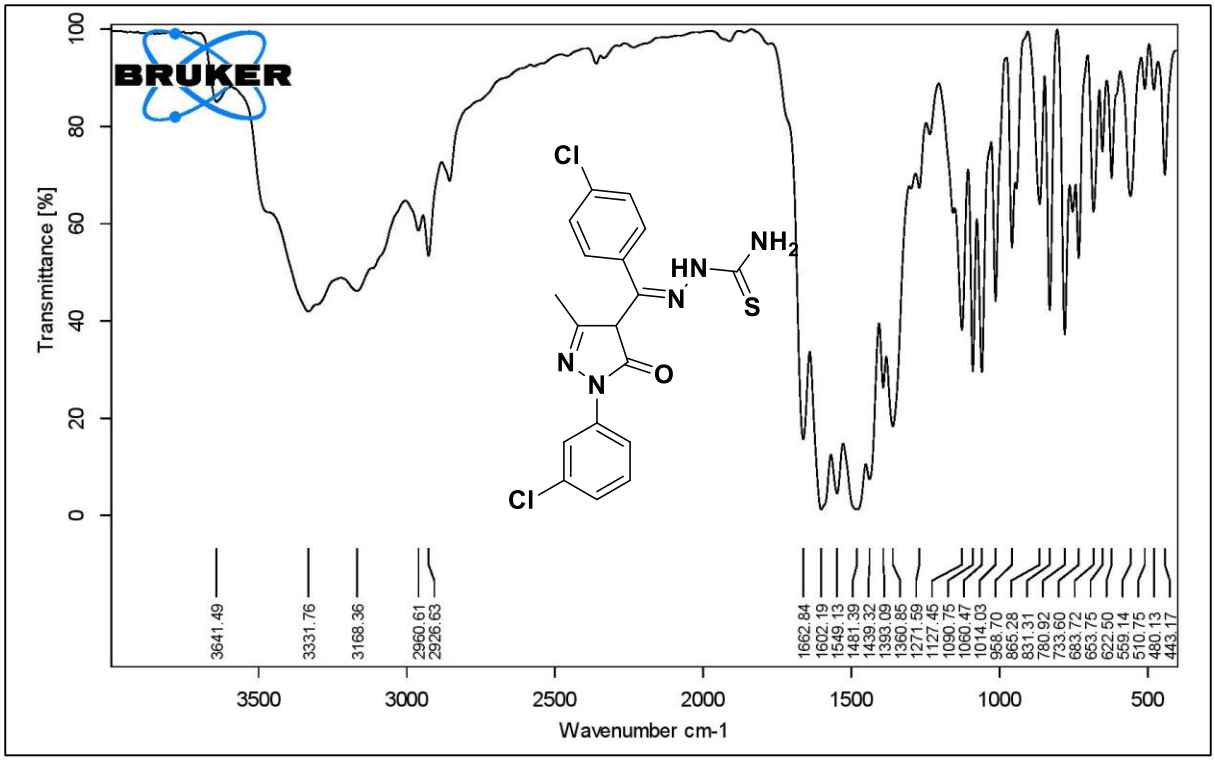

Fig. 4.10. FTIR spectrum of ligand **L9**.

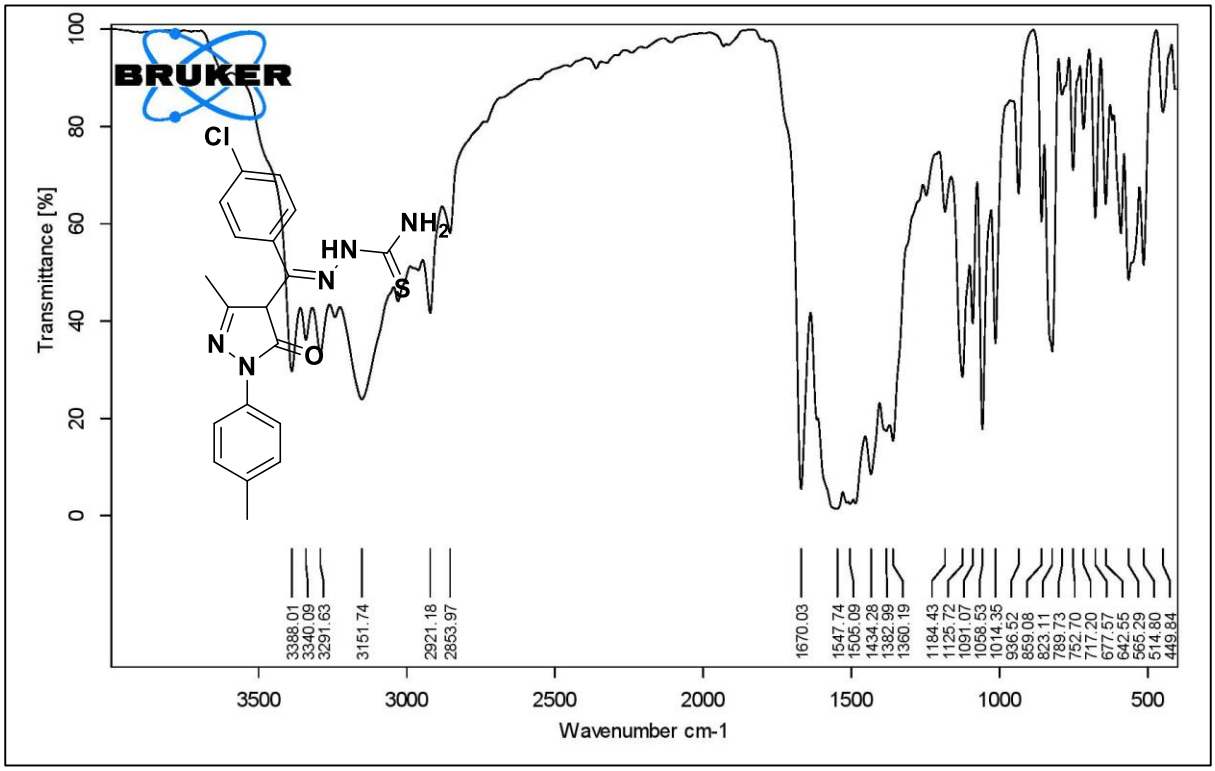

Fig. 4.11. FTIR spectrum of ligand **L10**.

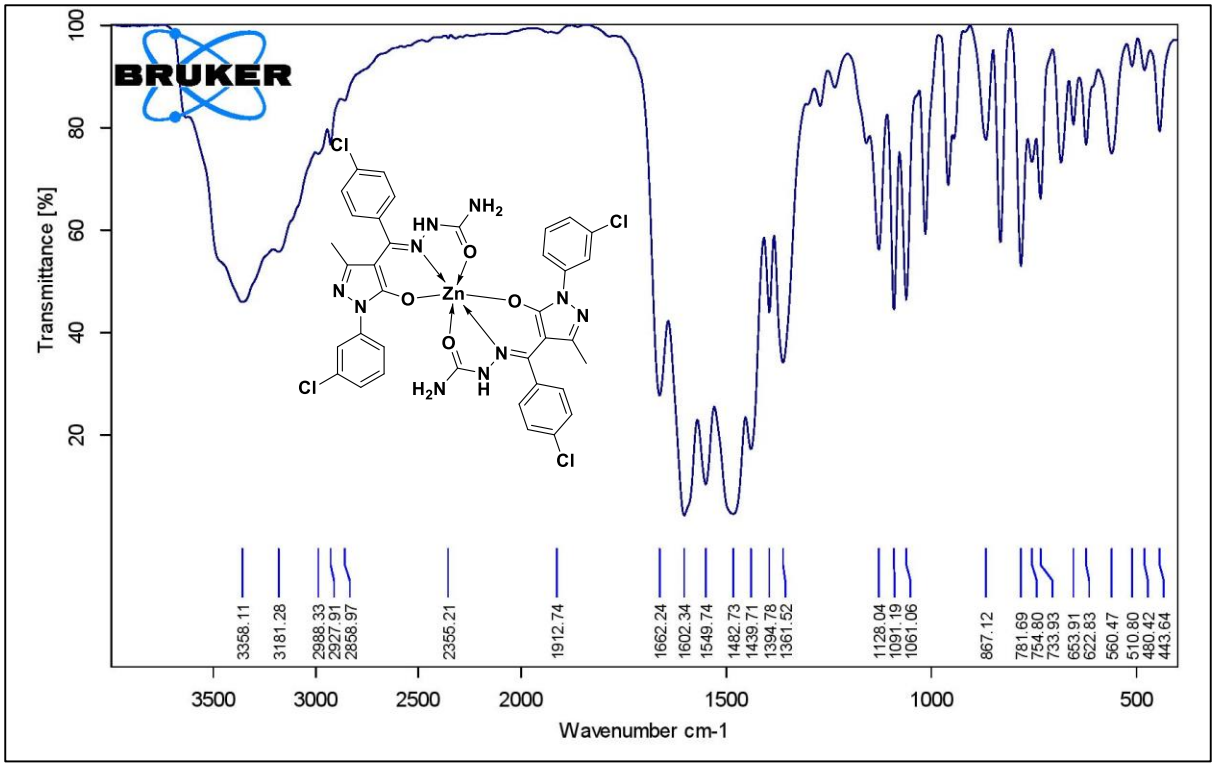

Fig. 4.12. FTIR spectrum of complex **19**.

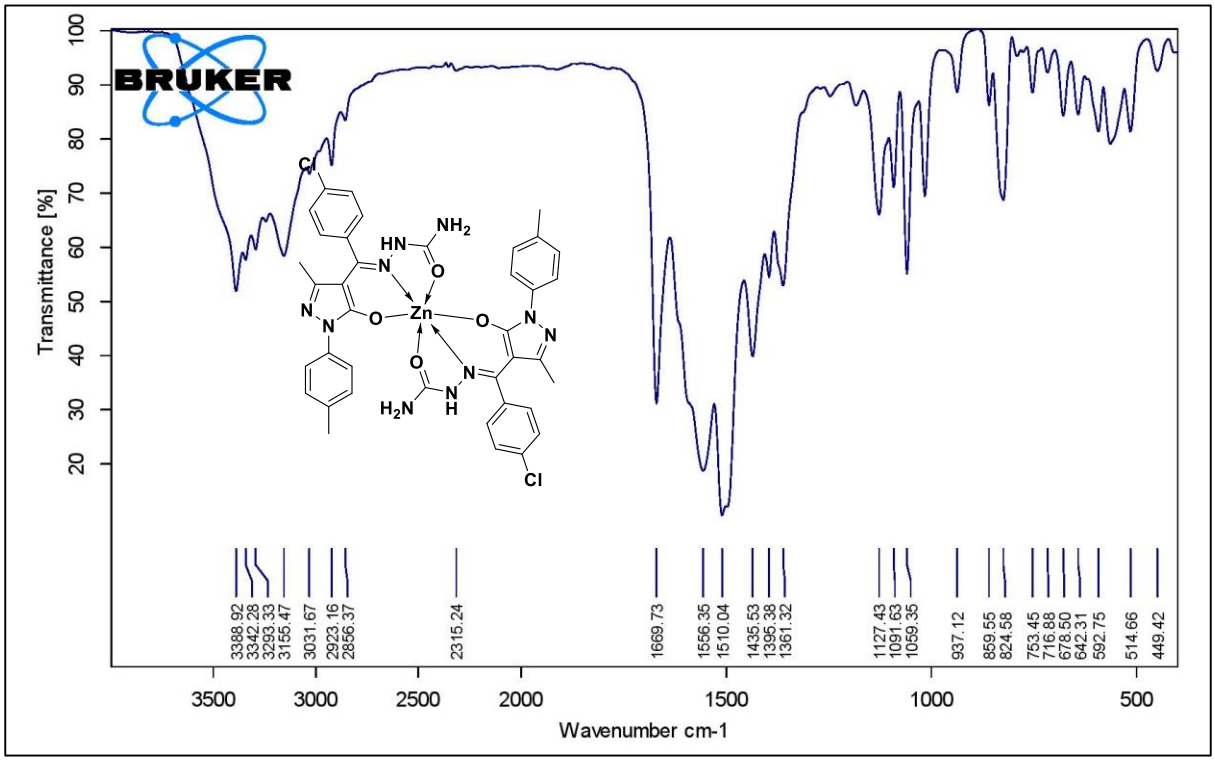

Fig. 4.13. FTIR spectrum of complex **20**.

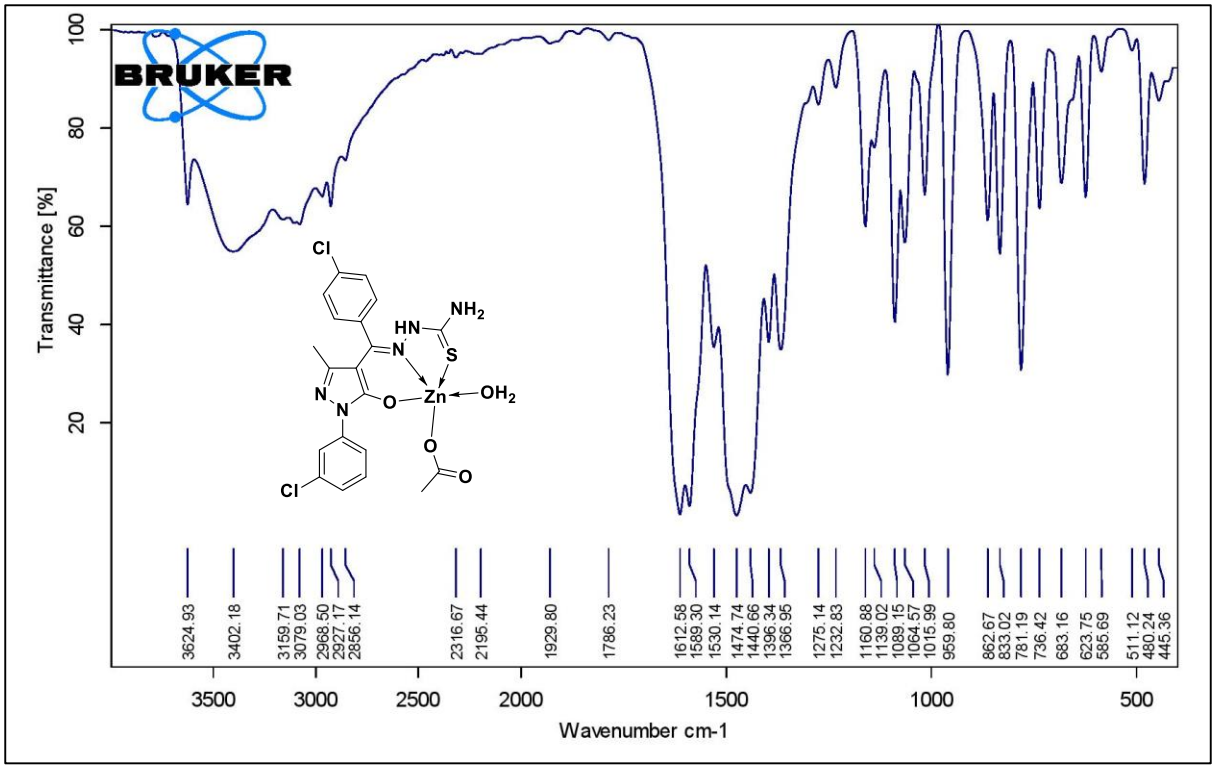

Fig. 4.14. FTIR spectrum of complex **21.**

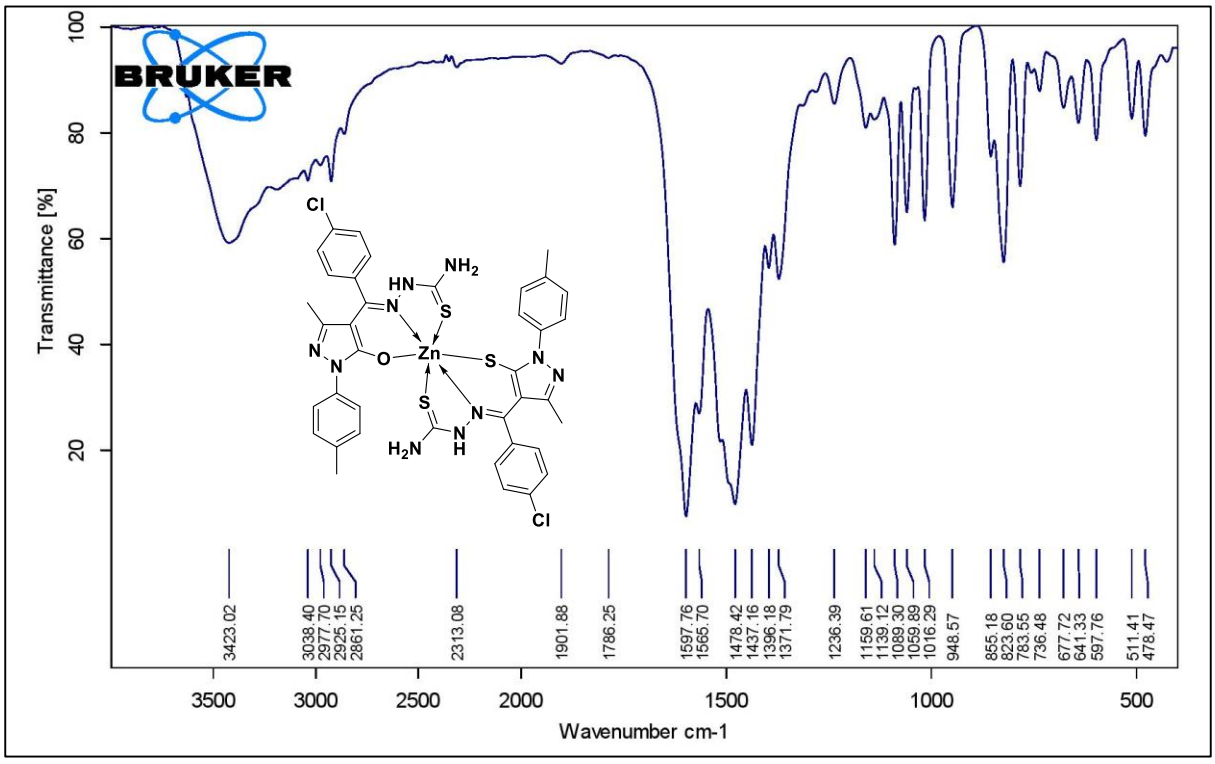

Fig. 4.15. FTIR spectrum of complex **22.**

4.3.3. ^{1}H NMR of compounds

In the ^{1}H NMR spectrum of ligand **L7**, The spectrum shows a singlet at 2.13 (3H) δ ppm confirm methyl group at C3 position of pyrazolone. All aromatic protons show signals at their expected aromatic region 7.19-7.96 δ ppm. For ligand **L8**, the spectrum shows two singlets in the aliphatic region at 2.13(3H) and 2.41 (3H) δ ppm for a methyl group of pyrazolone and *p*-tolyl group respectively. The spectrum shows a doublet of doublet in the aromatic region at 7.50-7.62 δ ppm confirms protons of *p*-chloro benzoyl moiety in the ligand. All other protons show signals at their expected region. In the ^{1}H NMR spectrum of ligand **L9**, the spectrum shows a singlet at 2.22 (3H) δ ppm for a methyl group of pyrazolone. The spectrum shows a doublet of doublet at 7.51-7.63 δ ppm for protons of *p*-chloro benzoyl of ligand moiety. All protons indicate signals at their expected regions. In the ^{1}H NMR spectrum of **L10**, the spectrum shows two singlets at 2.11 (3H) δ ppm and 2.41 (3H) δ ppm due to the methyl group of pyrazolone and tolyl respectively. A doublet of doublet at 7.49-7.62 (4H) δ ppm indicates *p*-chloro benzoyl of the ligand moiety. ^{1}H NMR spectra are presented in Fig. 4.16-4.21.

^{1}H NMR spectrum of complex **21**, the spectrum shows a singlet at 1.9 δ ppm of methyl protons of pyrazolone group. In the ^{1}H NMR spectrum of complex **22**, two singlets are observed at 1.7 and 2.3 δ ppm due to methyl and tolyl group respectively. All aromatic proton signals are obtained their expected region. ^{1}H NMR spectrum revealed formation of structure of complex **22.**

^{1}H NMR spectra of ligands:

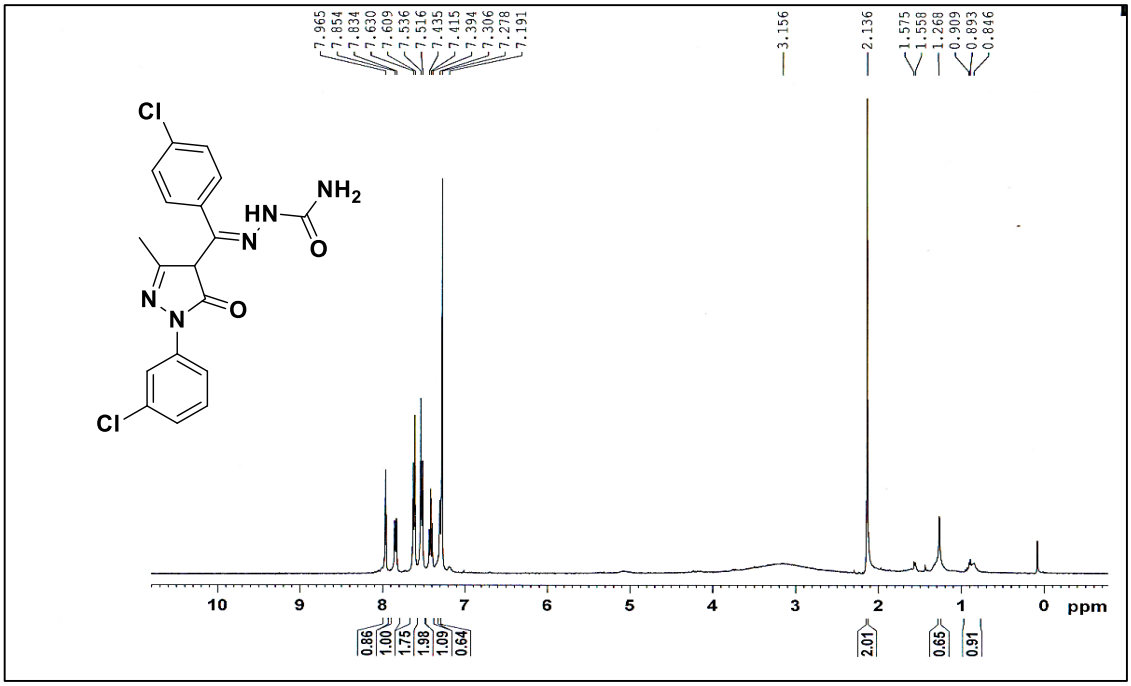

Fig. 4.16. ^{1}H NMR spectrum of ligand **L7**.

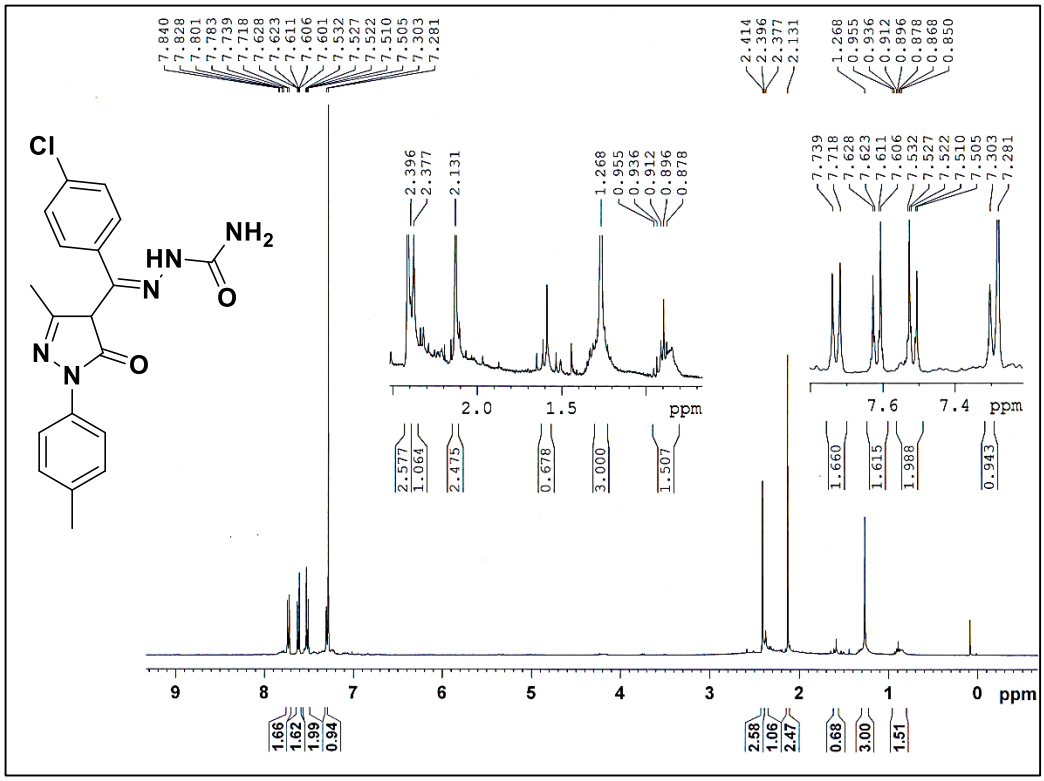

Fig. 4.17. ^{1}H NMR spectrum of ligand **L8**.

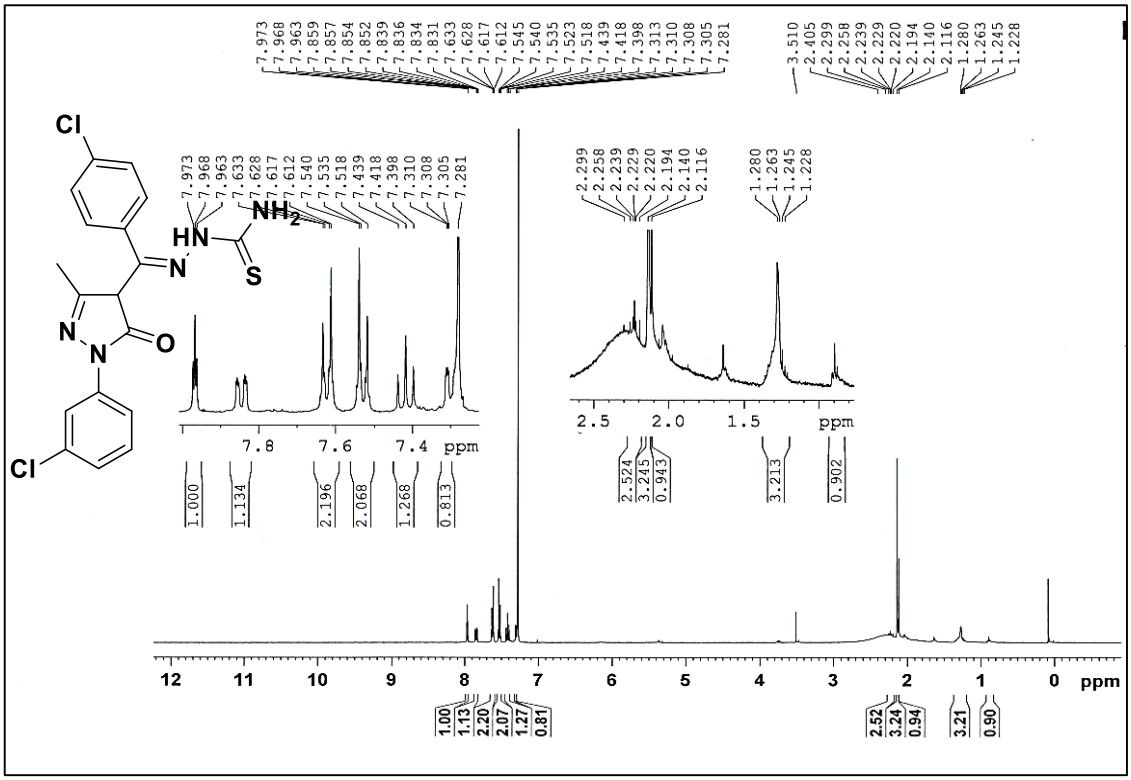

Fig. 4.18. ^{1}H NMR spectrum of ligand **L9**.

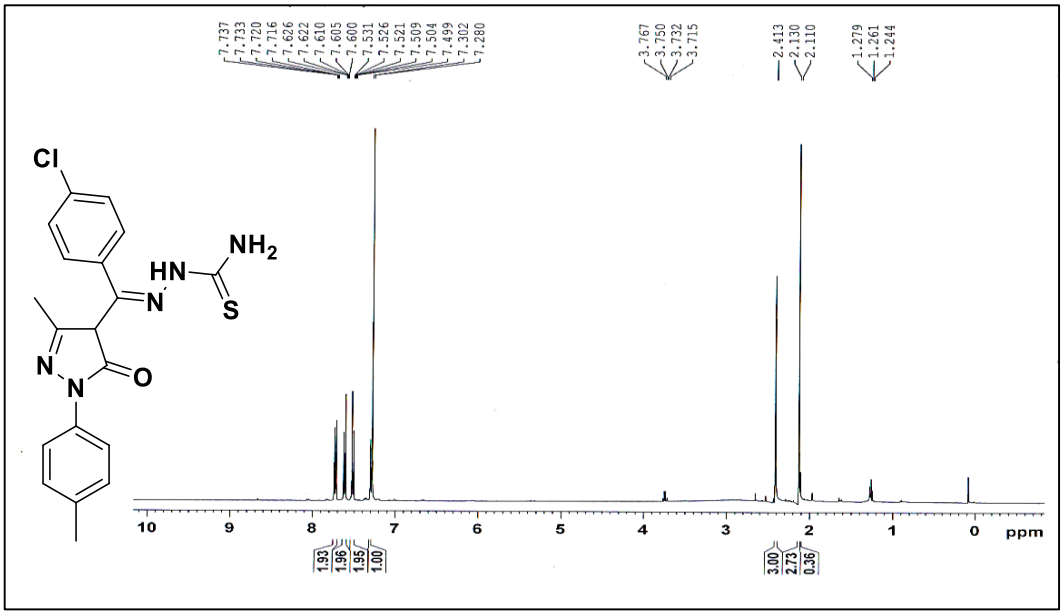

Fig. 4.19. ^{1}H NMR spectrum of ligand **L10**.

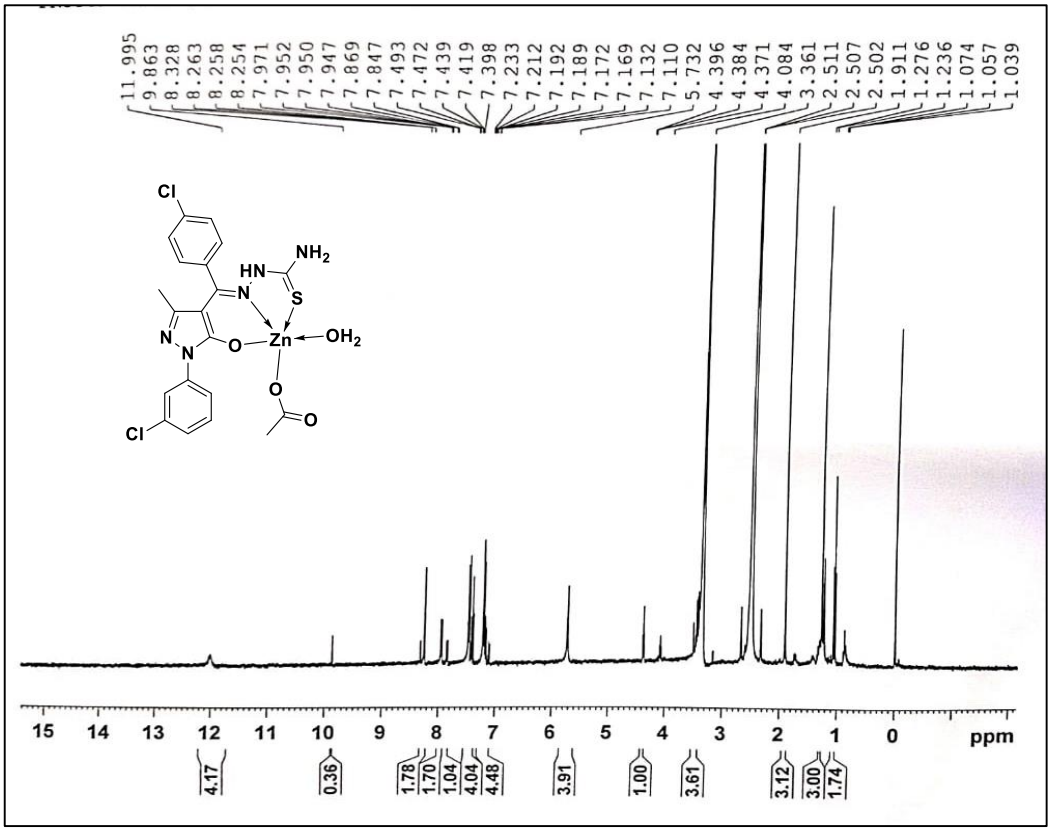

Fig. 4.20. ^{1}H NMR spectrum of complex 21.

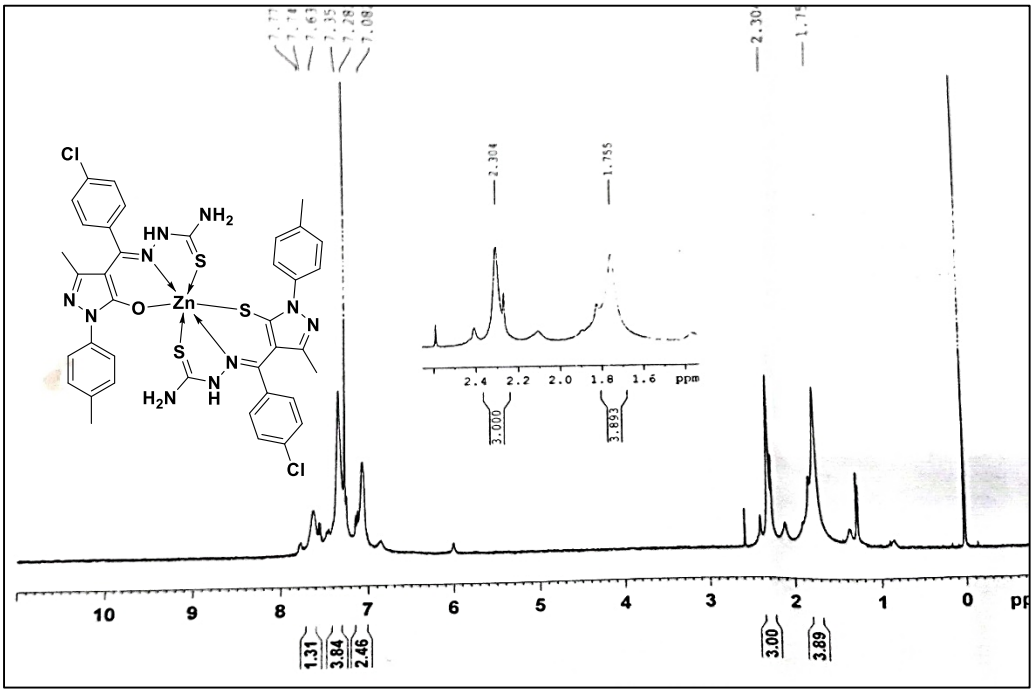

Fig. 4.21. ^{1}H NMR spectrm of complex **22**.

4.3.4. Electronic spectra of ligands and complexes

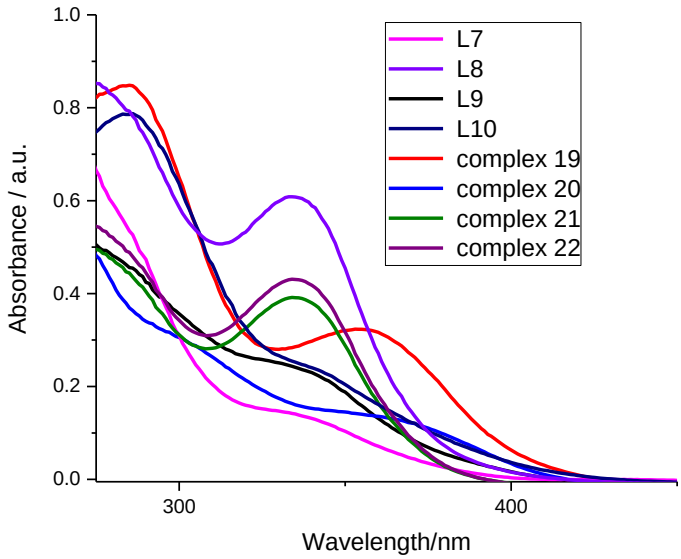

Fig. 4.22. Electronic spectra of ligands and complexes.

All complexes were completely soluble in DMSO and UV-Visible spectra were recorded in the range 250–500 nm of 10^{-6} molar solution of ligands and complexes (Fig. 4.22). In UV-Vis spectra of complexes, the first intense band is attributed to a ligand-centered (LC) π–π* transition localized on the aromatic rings of the ligand, while the shoulder is due to its metal coordination. There is no d-d transition in all complexes due to d^{10} metal. Spectra showed LMCT bands at around 330 nm in complexes.

4.3.5. Molar conductance of ligands and complexes

The conductivities of zinc(II) metal complexes and ligands in DMSO were measured with a calibrated conductivity cell at room temperature. The low conductivity values in DMSO reveal Complexes are non-electrolytic in nature. The conductivity of each solution (1×10^{-3} M) was measured and used for further calculations where possible, specific conductivities and molar conductivities (Table 4.5).[15,25]

$$\text{Sp. conductivity} = \text{cell constant} \times \text{conductivity}$$

$$\text{Molar conductivity} = \frac{\text{sp. conductivity} \times 1000}{\text{molarity of solution}}$$

Table 4.5. Molar conductance of ligands and complexes.[15]

Compound code	Λ_m ($s \cdot cm^2 \cdot mol^{-1}$)
L7	9.9
L8	5.7
L9	4.4
L10	7.7
[Zn(**L7**)$_2$] **19**	8.2
[Zn(**L8**)$_2$] **20**	4.2
[Zn(**L9**)(H_2O)(AcO)] **21**	3.3
[Zn(**L10**)$_2$] **22**	8.5

4.3.6. Cytotoxicity of zinc(II) complexes

4.3.6.1. Cytotoxicity of complex 19

Cytotoxicity of the synthesized zinc metal complex (**19**) was assessed against A549 cells by MTT assay. Doses 1, 5, 10, 25 and 50 µg/ml accounted for a weak cytotoxicity response with more than 70% cells being viable at the end of 24 h. But the subsequent doses of 100-1000 µg/ml accounted for 15% viability thus indicating at significant toxicity induced by the zinc(II) complex **19**. It is hypothesized in the present study that Zn (II) chelation by pyrazolone based semicarbazone ligand accounts for cytotoxicity observed herein.

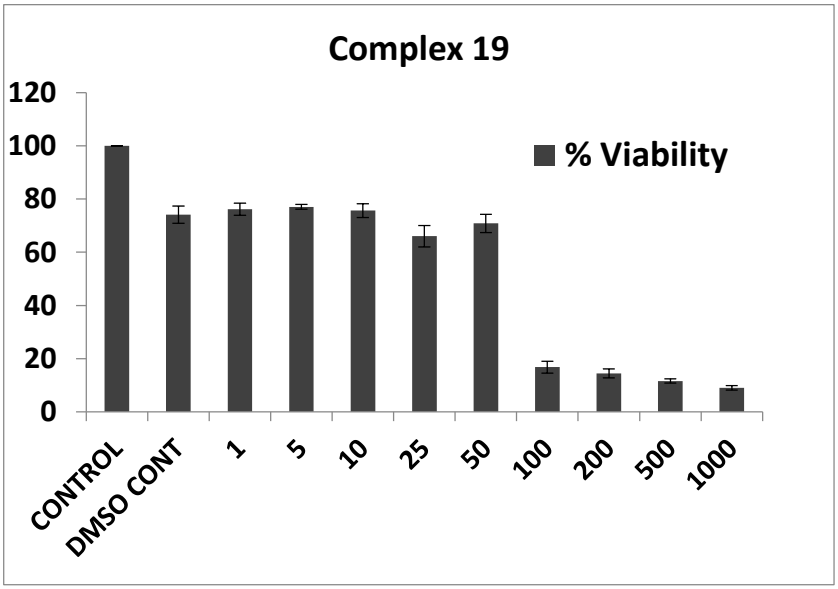

Fig. 4.23. Cytotoxicity against A549 lung cell by MTT assay of complex **19**.

MTT assay is focused at reporting the viability of a cell as a result of mitochondrial function and loss of viability is implicated on mitochondrial dysfunction (Thounaojam *et al*., 2011 &

Upadhyay *et al.*, 2018).[26,27] Results obtained herein suggest mitochondrial dysfunction induced by metal complexes results in loss of cell viability of A549 cells.[15]

4.3.6.2. Cytotoxicity of complex 20

Cytotoxicity of the synthesized metal complex was assessed against A549 cells by MTT assay. Doses 1, 5, 10, 25 and 50 µg/ml accounted for a weak cytotoxicity response with more than 70% cells being viable at the end of 24 h. But the subsequent doses of 100-1000 µg/ml accounted for 14% viability thus indicating at significant toxicity induced by the metal complex. It is hypothesized in the present study that Zn (II) chelation by pyrazolone based ligand accounts for cytotoxicity observed herein. MTT assay is focused at reporting the viability of a cell as a result of mitochondrial function and loss of viability is implicated on mitochondrial dysfunction (Thounaojam *et al.*, 2011 & Upadhyay *et al.*, 2018).[26,27] Results obtained herein suggest mitochondrial dysfunction induced by metal complexes results in loss of cell viability of A549 cells.[15]

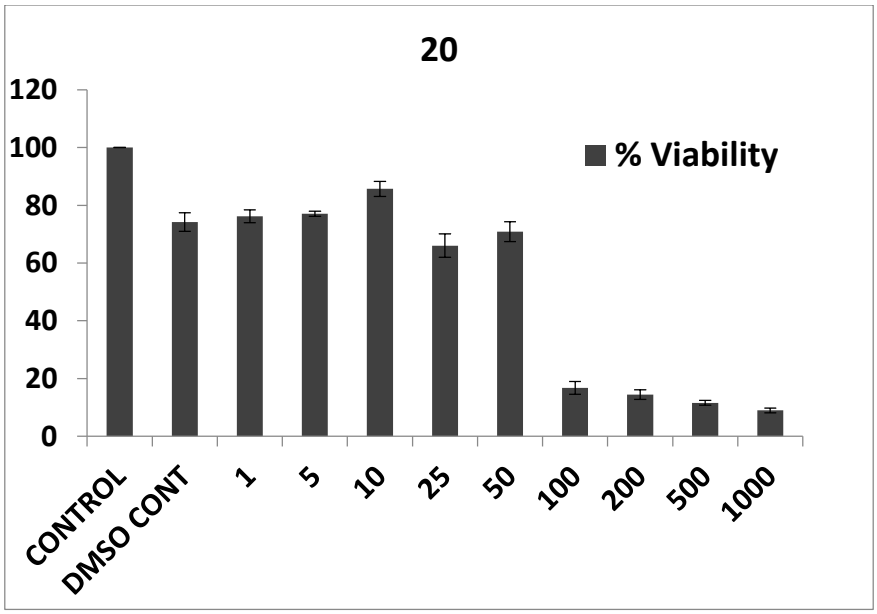

Fig. 4.24. Cytotoxicity against A549 cell by MTT assay of complex **20**.

4.3.6.3. Cytotoxicity of complex 21

Cytotoxicity of the synthesized metal complex was assessed against A549 cells by MTT assay.

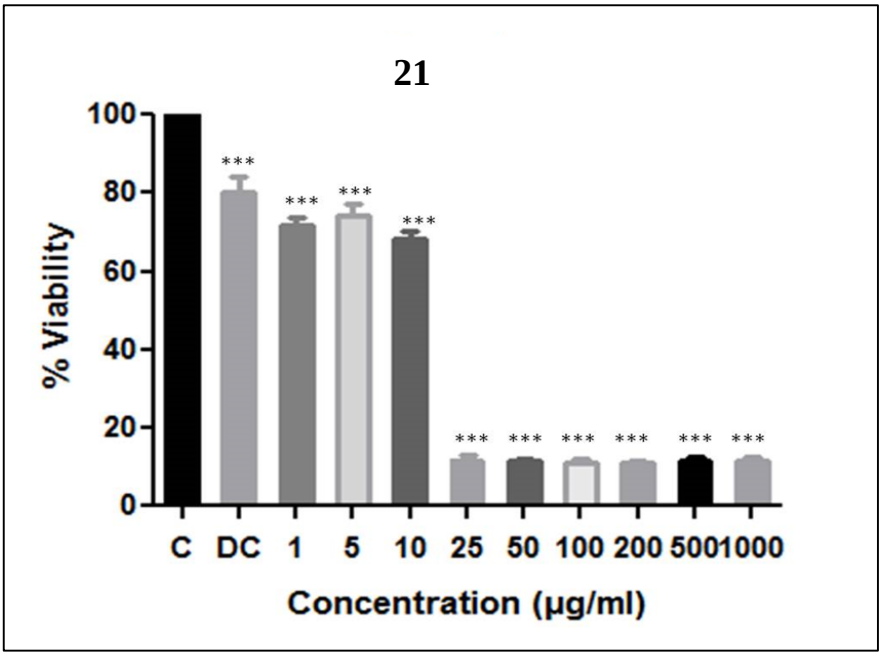

Fig. 4.25. Cytotoxicity against A549 cell by MTT assay of complex **21**.

Doses 1, 5 and 10 µg/ml accounted for a weak cytotoxicity response with more than 70% cells being viable at the end of 24 h. But the subsequent doses of 25-1000 µg/ml accounted for 11% viability thus indicating at significant toxicity induced by the metal complex. It is hypothesized in the present study that Zn (II) chelation by pyrazolone based ligand accounts for cytotoxicity observed herein. MTT assay is focused at reporting the viability of a cell as a result of mitochondrial function and loss of viability is implicated on mitochondrial dysfunction (Thounaojam *et al.,* 2011 & Upadhyay *et al.,* 2018).[26,27] Results obtained herein suggest mitochondrial dysfunction induced by metal complexes results in loss of cell viability of A549 cells.[15]

4.3.6.4. Cytotoxicity of complex 22

Cytotoxicity of the synthesized metal complex was assessed against A549 cells by MTT assay. Doses 1, 5 and 10 µg/ml accounted for a weak cytotoxicity response with more than 70% cells being viable at the end of 24 h. But the subsequent doses of 25-1000 µg/ml accounted for 10% viability thus indicating at significant toxicity induced by the metal complex. It is hypothesized in the present study that Zn (II) chelation by pyrazolone based ligand accounts for cytotoxicity observed herein. MTT assay is focused at reporting the viability of a cell as a result of mitochondrial function and loss of viability is implicated on mitochondrial dysfunction (Thounaojam *et al.,* 2011 & Upadhyay *et al.,* 2018).[26,27] Results obtained herein suggest

mitochondrial dysfunction induced by metal complexes results in loss of cell viability of A549 cells.[15]

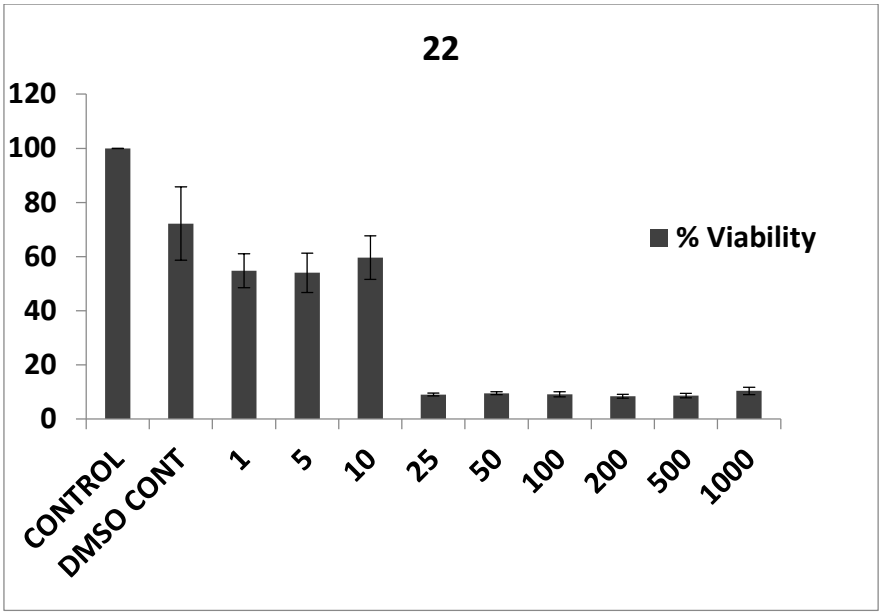

Fig. 4.26. Cytotoxicity against A549 cell by MTT assay of complex **22**.

Conclusion

Synthesized 4-semicarbazone -5-pyrazolones and 4-thiosemicarbazone-5-pyrazolones and well-characterized by ^{1}H NMR, FTIR, UV-Vis and X-ray diffraction spectroscopy. Zn(II) complexes of these ligands have been synthesized and characterized by modern spectroscopic technique with FTIR, UV/Vis spectroscopy, Elemental enalysis, Gravimetric and volumetric and Molar conductance. All complexes have been screened for MTT assay against A549 cell.

References

1 C. Dohutia, P. P. Kaishap and D. Chetia, *Artic. Int. J. Pharm. Pharm. Sci.*, 2012, **5**, 87–90.

2 F. Marchetti, C. Pettinari, C. Di Nicola, A. Tombesi and R. Pettinari, *Coord. Chem. Rev.*, 2019, **401**, 213069–213145.

3 G. I. Kornis, in *Kirk-Othmer Encyclopedia of Chemical Technology*, 2000.

4 Z. Zhao, X. Dai, C. Li, X. Wang, J. Tian, Y. Feng, J. Xie, C. Ma, Z. Nie, P. Fan, M. Qian, X. He, S. Wu, Y. Zhang and X. Zheng, *Eur. J. Med. Chem.*, 2020, **186**, 111893–111918.

5 K. J. Nakum and R. N. Jadeja, *Zeitschrift für Naturforsch. B*, 2018, **73**, 713–718.

6 K. M. Vyas, V. K. Shah and R. N. Jadeja, *J. Coord. Chem.*, 2011, **64**, 1069–1081.

7 B. Kumar, K. J. Nakum, R. N. Jadeja, R. Kant and V. K. Gupta, *Acta Crystallogr. Sect. E*, 2015, **71**, 280–281.

8 R. N. Jadeja, K. M. Vyas, K. K. Upadhyay and R. V. Devkar, *RSC Adv.*, 2017, **7**, 17107–17116.

9 R. N. Jadeja, K. M. Vyas, V. K. Gupta, R. G. Joshi and C. Ratna Prabha, *Polyhedron*, 2012, **31**, 767–778.

10 R. N. Jadeja, M. Chhatrola and V. K. Gupta, *Polyhedron*, 2013, **63**, 117–126.

11 Y. Yang, D. Wu, D. Jia, L. Liu and A. Liu, *Int. J. Quantum Chem.*, 2011, **111**, 1048–1054.

12 K. M. Vyas, R. G. Joshi, R. N. Jadeja, C. Ratna Prabha and V. K. Gupta, *Spectrochim. Acta - Part A Mol. Biomol. Spectrosc.*, 2011, **84**, 256–268.

13 J. N. Asegbeloyin, E. C. Okafor, N. N. Ukwueze, I. Babahan and I. C. Agbo, *Asian J. Chem.*, 2014, **26**, 2753–2758.

14 E. Pahonţu, F. Julea, Y. Chumakov, P. Petrenco, T. Roşu and A. Gulea, *J. Organomet. Chem.*, 2017, **836**, 44–55.

15 I. Shaikh, A. Vohra, R. Devkar and R. Jadeja, *Eur. J. Chem.*, 2019, **10**, 131–138.

16 University of Gottingen, *G.M. Sheldrick, SHELXS97 and SHELXL97*, Germany, 1997.

17 G. M. Sheldrick, *Acta Crystallogr. Sect. A Found. Crystallogr.*, 2015, **71**, 3–8.

18 O. V. Dolomanov, L. J. Bourhis, R. J. Gildea, J. A. K. Howard and H. Puschmann, *J. Appl. Crystallogr.*, 2009, **42**, 339–341.

19 A. L. Spek, *J. Appl. Crystallogr.*, 2003, **36**, 7–13.

20 M. Nardelli, *J. Appl. Crystallogr.*, 1995, **28**, 659–665.

21 G. M. Sheldrick, *Acta Crystallogr. Sect. A Found. Crystallogr.*, 2008, **64**, 112–122.

22 C. F. MacRae, I. Sovago, S. J. Cottrell, P. T. A. Galek, P. McCabe, E. Pidcock, M. Platings, G. P. Shields, J. S. Stevens, M. Towler and P. A. Wood, *J. Appl. Crystallogr.*, 2020, **53**, 226–235.

23 I. Shaikh, R. N. Jadeja and R. Patel, *Polyhedron*, 2020, **183**, 114528.

24 A. W. Addison, T. N. Rao, J. Reedijk, J. van Rijn and G. C. Verschoor, *J. Chem. Soc. Dalt. Trans.*, 1984, 1349–1356.

25 W. J. Geary, *Coord. Chem. Rev.*, 1971, **7**, 81–122.

26 M. C. Thounaojam, R. N. Jadeja, M. Valodkar, P. S. Nagar, R. V. Devkar and S. Thakore, *Food Chem. Toxicol.*, 2011, **49**, 2990–2996.

27 K. K. Upadhyay, R. N. Jadeja, J. M. Thadani, A. Joshi, A. Vohra, V. Mevada, R. Patel, S. Khurana and R. V Devkar, *Toxicol. Appl. Pharmacol.*, 2018, **360**, 99–108.

Published Paper:

European Journal of Chemistry 10 (2) (2019) 131-138

European Journal of Chemistry

Check for updates

View Journal Online
View Article Online

Synthesis, characterization, structural features and cytotoxicity of innovative zinc(II) complex derived from ONS-donor thio-Schiff base of acyl pyrazolone

Irfan Shaikh [1], Aliasgar Vohra [2], Ranjitsinh Devkar [2] and Rajendrasinh Jadeja [1]

[1] *Department of Chemistry, Faculty of Science, The Maharaja Sayajirao University of Baroda, Vadodara-390002, India*
irfan.chemistry7@gmail.com (I.S.), rjadeja-chem@msubaroda.ac.in (R.J.)
[2] *Department of Zoology, Faculty of Science, The Maharaja Sayajirao University of Baroda, Vadodara 390 002, India*
aliasgarvohra@rocketmail.com (A.V.), phyto_met@yahoo.com (R.D.)

* *Corresponding author at: Department of Chemistry, Faculty of Science, The Maharaja Sayajirao University of Baroda, Vadodara-390002, India. Tel: +91.0265.2795552 Fax: +91.0265.2795552 e-mail: rjadeja-chem@msubaroda.ac.in (R. Jadeja).*

RESEARCH ARTICLE

10.5155/eurjchem.10.2.131-138.1858

Received: 29 March 2019
Received in revised form: 09 May 2019
Accepted: 10 May 2019
Published online: 30 June 2019
Printed: 30 June 2019

KEYWORDS

ONS donors
Cytotoxicity
Zn(II) complex
Thio-Schiff base
Single crystal structure
Acyl pyrazolone derivatives

ABSTRACT

Novel acyl pyrazolone and thio-Schiff base of acyl pyrazolone ligand HL (2-((4-chlorophenyl)(1-(3-chlorophenyl)-3-methyl-5-oxo-4,5-dihydro-1*H*-pyrazol-4-yl)methylene) hydrazine-1-carbothioamide) has been synthesised and characterized by FT-IR and ^{1}H NMR techniques. This unusual coordinated complex $[Zn(L)(CH_3C00)(H_2O)]CH_3CH_2OH$ has been synthesized and characterized by FT-IR, thermogravimetric analysis (TGA), UV-Vis spectroscopy and single crystal X-ray diffraction. ^{1}H NMR confirms the structure of the thio-Schiff base used in the study. The structural data reveal that mononuclear Zn(II)complex has distorted square pyramidal geometry. S-S interaction, Inter molecular and intra molecular H-Bond found in crystal packing of the complex. The complex has been screened for MTT assay against A549 cell lines. The Zn(II) complex is cytotoxic against the screened cell line at low concentration.

Cite this: *Eur. J. Chem.* **2019**, *10(2)*, 131-138 **Journal website**: www.eurjchem.com

1. Introduction

The Schiff based ligands of acyl pyrazolones paying attention in recent time due to its coordination ability and decent biological activities [1-6]. Reaction between ketones (or aldehydes) and a thiosemicarbazide that gives thiosemicarbazones and which are called thio-Schiff and owing to their good binding capacity to metal they are very suitable in coordination chemistry [7]. Tautomer thione (-C=S) and thiol (-C-SH) forms (Figure 1) of thiosemicarbazone act as neutral or anionic bidentate ligands from the donor sites of azomethine N and S(thione/thiol) [8,9].

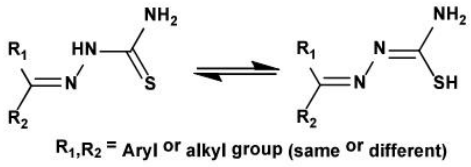

Figure 1. Thione, thiol tautomer of thiosemicarbazone.

Their Zn (II) complexes show prospective fluorescence properties [10,11]. Several metal complexes showed respectable biological activities with significant thiosemicarbazone of acyl pyrazolone [12]. Selected metal complexes of thiosemicarbazone are octahedral, square planer, square pyramidal and trigonal bipyramidal are reported in recent time [12,13].Very unique binding from three different molecules, penta coordinated square pyramidal geometry of thio-Schiff Zn(II) complex is reported in this article.

Metal complexes of thio-Schiff base ligands appreciated because of their antimicrobial, antifungal, antioxidant and catalytic activities [14-17]. Metal complexes of tridentate acyl pyrazolone based thiosemicarbazone showed some decent results of several bioactivities [12]. Herein, zinc(II) complex of thio-Schiff base of biological active acyl pyrazolone synthesized and reported sound result of cytotoxicity againstA549 cells by MTT assay.

2. Experimental

2.1. Materials

European Journal of Chemistry
ISSN 2153-2249 (Print) / ISSN 2153-2257 (Online)
http://dx.doi.org/10.5155/eurjchem.10.2.131-138.1858